To the Graduate Council:

I am submitting herewith a thesis written by Paul Nicholson Horne entitled "Immobilization of Clostridium thermocellum Bacterium on Coal Particles for Cellulosic Biomass Conversion." I have examined the final copy of this thesis for form and content and recommend that it be accepted in partial fulfillment of the requirements for the degree of Master of Science, with a major in Chemical Engineering.

H. W. Hsu

H. W. Hsu, Major Professor

We have read this thesis and recommend its acceptance:

George C. Frazier

Accepted for the Council:

L. Evans Haak

Vice Chancellor
Graduate Studies and Research

IMMOBILIZATION OF *CLOSTRIDIUM THERMOCELLUM* BACTERIUM ON COAL PARTICLES FOR CELLULOSIC BIOMASS CONVERSION

A Thesis

Presented for the

Master of Science

Degree

The University of Tennessee, Knoxville

Paul Nicholson Horne

March 1982

ACKNOWLEDGMENTS

The author wishes to express his appreciation to several people whose assistance was instrumental in the completion of this study:

- Dr. H. W. Hsu, for his guidance and advice throughout the course of this study;
- Dr. H. F. Johnson and the Department of Chemical, Metallurgical and Polymer Engineering for financial support of the project;
- Dr. D. C. Bogue and Dr. G. C. Frazier, for serving on the M.S. committee;
- Dr. J. O. Mundt, for technical advice and use of laboratory equipment;
- Mr. and Mrs. Paul J. Horne, for their continuing support and encouragement.

ABSTRACT

The adsorption isotherms of Clostridium thermocellum cells on bituminous coal particles of approximately 0.15-0.18 mm diameter were determined at 60°C, 45°C, and 30°C with a pH value of 7.0, and at 60°C with pH values of 6.0 and 5.0. The adsorption data were correlated with a Langmuir isotherm that was modified to account for a reduction in repulsive interaction potential at lower concentrations of adsorbed cells.

From the temperature coefficients of the equilibrium constant, the thermodynamic quantities of Gibbs free energy, ΔG, enthalpy, ΔH, and entropy, ΔS, were estimated. The enthalpy change, ΔH, was found to be in the range between -1.43 Kcal/gmol at higher cellular concentrations and -1.78 Kcal/gmol at lower concentrations which indicated that the bacterial adsorption was exothermic. The Gibbs free energy changes, ΔG, were found to be in the range between -1.74 Kcal/gmol and -0.21 Kcal/gmol indicating that adsorption was thermodynamically favorable. Free energy changes for adsorption at pH values of 6.0 and 5.0 were significantly reduced at high immobilized cell concentrations.

TABLE OF CONTENTS

CHAPTER PAGE

LIST OF TABLES

LIST OF FIGURES

FIGURE PAGE

CHAPTER I

INTRODUCTION

Successful utilization of cellulosic materials as a long range solution to our resources problem of energy and chemicals depends on the development of economically feasible process technologies. Microbiological processing of cellulosic biomass is desirable since it is generally more efficient and less energy intensive than chemical hydrolysis and synthesis. Clostridium thermocellum is an anaerobic, thermophilic bacterium capable of hydrolyzing cellulose and fermenting the hexose hydrosylates to primarily ethanol, acetic acid, hydrogen and carbon dioxide. Continuous heterogeneous enzyme reactions by immobilized microbial cells represent a novel approach to established fermentation processes. In order to evaluate the potential for developing such an immobilized cell bioreactor for cellulosic biomass conversion, the adsorption of C. thermocellum cells to bituminous coal particles was studied.

Of the several methods of whole cell immobilization, bacterial adsorption is perhaps the simplest to implement. Coal was chosen over other adsorbents because of its availability and reported use in an immobilized cell bioreactor (33). If the adsorption process is of the usual type, it should follow one of the classical isotherms described by parameters related to the limiting capacity and equilibrium constant of adsorption. In this study, the bacteria-coal adsorption equilibria were analyzed in terms of thermodynamic properties in order to examine the mechanism of adsorption.

CHAPTER II

OBJECTIVES AND SIGNIFICANCE

A. Objective of the Investigation

In the study of adsorption of solute from solution onto a solid surface, the following aspects are of greatest interest and importance:

1. the shape of the adsorption isotherm and the possibility of fitting it with an appropriate equation to represent a model
2. the significance of the adsorption limit
3. the adsorption coefficient
4. a consideration of the adsorption mechanism
5. the effect of temperature and pH on adsorption.

The objectives of this study were to study quantitatively the adsorption isotherms of C. thermocellum cells on bituminous coal particles.

B. Significance of Clostridium thermocellum as Biocatalyst for Cellulosic Biomass Conversion

There are several advantages of using C. thermocellum as the biocatalyst in the conversion of cellulosic materials. The bacterium is an obligate thermophile and displays a temperature optimum for growth near 60°C. Thermophiles possess high metabolic rates, thermally resistant and chemically stable enzymes, and they have a higher end product-to-cell ratio than is found in metabolically similar mesophilic species (45). At lower temperatures they remain viable and their functions are preserved although metabolic activity is reduced.

Fermentations at thermophilic temperatures also prevent the accumulation of known bacterial and viral pathogens and are, in general, more sanitary (11).

The engineering advantages of increased temperature operations are clear. Less energy is required for mixing and product recovery because of lower viscosity and surface tension, and higher vapor pressure. The increased solubility of organic compounds at higher temperatures is also a positive attribute because substrate solubility is often the rate-limiting step in the conversion of biopolymers. Further, the low activity and high stability of thermophilic cells and enzymes at room temperature places less stringent requirements on enzyme or cell recovery, and provides catalytic activity with a longer half-life for developing immobilization technology (45).

Anaerobic fermentations form the basis for microbial production of chemicals and fuels since, in the absence of oxygen, several reduced organic compounds are produced instead of the aerobic combustion products, carbon dioxide and water. Oxygen is lethal to certain anaerobes, however in the case of this Clostridium species, it only inhibits metabolism when exposure is limited to brief periods (5,45). This oxygen sensitivity does not present problems in large scale processing because oxygen is poorly soluble and readily removed, especially at thermophilic temperatures. Indeed, fermenter design is simpler in anaerobic processes since oxygen-related mass transfer problems are not encountered (44).

Use of C. thermocellum offers a direct approach to biomass utilization in that cellulase production, cellulose hydrolysis, and fermentation of the hydrolysis products can be achieved in a single processing step. The growth of the bacterium on cellulose results in the production of an extracellular cellulase complex with glucose and cellobiose as the major, long-term hydrolysis products (17,29). The cellulase complex is stable, easily recoverable and is produced in high yield (3,29). C. thermocellum displays the highest cellulolytic activity among the anaerobes and its growth rate on cellulose or cellobiose is greater than that of Trichoderma virde, the fungus commonly associated with efficient and rapid cellulose hydrolysis (44). It is significant that the hydrolysis products of cellulose do not inhibit the production of the cellulase as is the case in all other microbial cellulases (17,35). The metabolism of these hydrolysis products is often a rate-limiting step in the bioconversion of cellulose, therefore the lack of catabolite repression is a considerable advantage over all other microbial cellulases.

C. Significance of Immobilized Cell Bioreactor

Biological reactions are generally slow and selection of the most efficient reactor type is important. The primary reasons for developing an immobilized cell bioreactor are to allow for the reuse of the microorganisms, to maintain high cell populations for fast reaction rates and greater productivities, and to make a batch process continuous (1,39). Higher conversion efficiencies and higher yields for substrates undergoing product inhibition are possible when

plug-flow reactors are utilized over continuous flow stirred-tank reactors (7,25). Immobilized cells are stable and generally less subject to the effects of inhibitory compounds and nutrient depletion (1). Maintaining the cells at a desired physiological state is possible and this may contribute to the formation of certain cell products. It also decreases or eliminates non-productive lag or growth phases. Higher productivities can be achieved since the reactor can be operated at high dilution rates without washout (36,39). Since the bacteria are concentrated on a solid surface, fluid viscosity is lower and mixing and mass transfer are improved.

When compared to immobilized enzymes, immobilized cells have the advantage of not requiring enzyme isolation and purification or co-factor regeneration (20). The use of the entire cell has greater potential for multi-step processes and maintains the enzyme in its native state (1).

CHAPTER III

LITERATURE REVIEW

A. Clostridium thermocellum

Characteristics and physiology. The desirable process features of fermentations by C. thermocellum have been the impetus for detailed studies, both basic (10,27,29,42) and applied (16) on the conversion of cellulose to ethanol and other useful products. Some of the important characteristics of the bacterium are listed in Figure 1. The ability to ferment certain substrates and the relative amounts of the end products are strain specific properties. Figure 2 indicates the metabolic pathways involved in the catabolism of cellulose by C. thermocellum. The activities of the extracellular cellulases appear to be coordinated with the saccharide transport activities since the bacterium contains both a cellobiose phosphorylase and a cellodextrin phosphorylase (44). Hence, the primary hydrolytic products are activated to glucose-1-phosphate without expenditure of ATP. The phosphoroclastic pathway is employed intracellularly for the generation of ethanol, acetic and lactic acids, hydrogen and carbon dioxide (44). In some strains, butyric acid is produced near the end of fermentation. The faster rate of growth of C. thermocellum on cellobiose than on cellulose and the accumulation of hydrolysis products suggest that both cellulose hydrolysis and the uptake of the hydrosylates are rate-limiting steps in the pathway (10,40,42).

Common Habitat:[2] Widely dispersed in soils

Source:[2] Horse and bovine manure, human feces, soil, marine mud

Morphology:[2,3]

Vegetative forms--rods approximately 0.6 μ x 4 μ, straight or slightly curved, usually occur as individuals, motile with lateral flagella
Spores--terminally oval approximately 1.2 μ x 1.6 μ

Gram Stain:[2,3] Negative

Growth Temperature:[1,2,3] Grows 50°C-68°C, optima 60°C-64°C

Obligate Anaerobe:[1,2,3] Sensitivity to oxygen not extreme

Growth Substrates:[3] Cellulose and its derivatives, cellobiose; no growth on glucose

Primary Fermentation Products:[2,3] Ethanol, acetic acid, lactic acid, H_2, CO_2

Maximum Specific Growth Rate:[3]
On cellulose--0.1 hr^{-1} (6.9 hr doubling time)
On cellobiose--0.3 hr^{-1} (2.3 hr doubling time)

Cellobiose Agar Surface Colonies:[2] Watery, slightly convex, translucent with bluish fluorescence

FIGURE 1

Characteristics of Clostridium thermocellum

[1]Garcia-Martinez, D. V., A. Shinmyo, A. Madia, and A. L. Demain, "Studies on Cellulase Production by Clostridium thermocellum," Eur. J. Appl. Microbiol. Biotechnol., 9, 189-197 (1980).

[2]McBee, R. H., "The Characteristics of Clostridium thermocellum," J. Bacteriol., 67, 505-506 (1954).

[3]Ng, T. K., P. J. Weimer, and J. G. Zeikus, "Cellulolytic and Physiological Properties of Clostridium thermocellum," Arch. Microbiol., 114, 1-7 (1977).

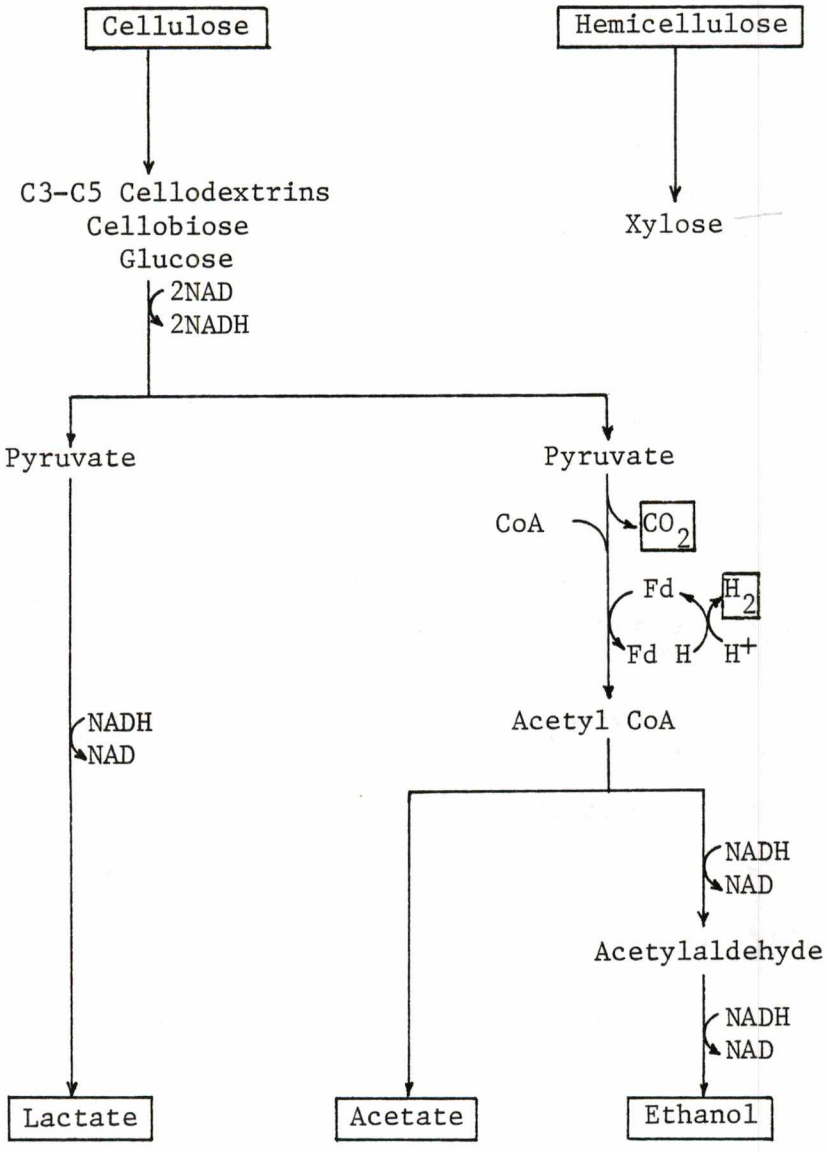

FIGURE 2

Fermentation Pathways of Clostridium thermocellum[1]

[1]Zeikus, J. G., "Chemical and Fuel Production by Anaerobic Bacteria," Ann. Rev. Microbiol., 34, 423-464 (1980).

Strain improvements. The physiology of several strains of C. thermocellum, both wild type and selected, have been studied. Strains ATCC 27405 and LQ8 have served as the parent cultures in the development of physiologically more desirable strains. The parent strains have similar properties including the ability to ferment only cellulose and cellodextrins; however, strain LQ8 exhibits a higher end product ethanol-to-acetate ratio which is approximately unity for ATCC 27405 (10,29,42). Both strains are incapable of growth on xylose and lack the ability to use glucose as a carbon source. Strain LQR1 has been isolated from a contaminated culture of LQ8 and differs in that glucose is fermented in high yeast extract medium, butyrate is not produced as an end product, and extracellular carboxymethylcellulose is produced when growth is on cellobiose or glucose (24,28). A cellulase-over-producing mutant strain, AS-39, has been isolated after UV irradiation of ATCC 27405 (17,35). Titers of both endo-β-glucanase and exo-β-glucanase of the cellulase complex have been found to double in a single mutagenesis step. This is encouraging since exo-β-glucanase activity is rather low in C. thermocellum (35). Strain AS-39 also has a higher ethanol-to-hydrogen fermentation product ratio than strain LQR1 (24).

At present, the major industrial drawback to the fermentative use of C. thermocellum is the low concentration (but not substrate-to-product yield) of ethanol tolerated and therefore produced (45). In the case of the parent strains, fermentation typically ceases when ethanol concentrations reach 0.8 g/l and the maximum amount of ethanol

tolerated is always less than one volume percent (10,29,42). Strain selection has resulted in cultures that can withstand up to five volume percent ethanol (10,19,40). It is important that the metabolism of these ethanol-tolerant strains is altered such that the ethanol-to-acetate product ratio is significantly increased (6,40). It is postulated that this new strain, S-6, produces very little hydrogen gas thereby shifting the reducing power to NADH production and ethanol generation (40). This strain also shows a high conversion efficiency--100% cellulose degradation when grown on Solka Floc (a delignified pulp derivative containing both cellulose and hemicellulose fractions) and an overall yield of 0.44 grams of product per gram of cellulose. Fermentation did not cease until the final ethanol and acetate concentrations were 8 g/l and 1.0 g/l, respectively, with 6 g/l of reducing sugars accumulated.

Mixed culture process developments. The cellulase enzyme complex from C. thermocellum is equally effective in the hydrolysis of hemicellulose in biomass to xylose as compared to cellulose hydrolysis. However, it cannot ferment xylose. Bacteria with the ability to ferment the hexose hydrosylates as well as pentoses have been included in stable mixed cultures to augment the fermentative capacity and to complement the superior cellulolytic properties of C. thermocellum. Clostridium thermosaccharolyticum is capable of catabolizing xylose, glucose, and cellobiose, and is biologically compatible with C. thermocellum (6,40). Fermentations by a mixed culture of these two bacteria have resulted in 100% degradation of Solka Floc (40). No reducing

sugars accumulated and the catabolic products were 15 g/l ethanol and 5 g/l acetate. The conversion efficiency from this fermentation was calculated to be 0.57 grams of product per gram of cellulose. In addition, enhanced yield from fermentation on corn stover has also been reported (40). This same mixed culture has also been applied to the direct conversion of SO_2/steam pretreated hardwood to ethanol (6). A preliminary cost analysis has estimated ethanol costs of about \$1.06/gallon for a 30 X 10^6 gallon/year plant producing 95 volume percent ethanol from poplar wood.

Another anaerobic thermophile, Clostridium thermohydrosulfuricum, has also been grown in co-culture with C. thermocellum (28). This bacterium can ferment glucose, cellobiose, and xylose, but not cellulose or xylan. This system appears to be an improvement over the previously mentioned mixed culture because of the enhanced rate of saccharide degradation and a higher ethanol yield. The co-culture actively ferments MN300 cellulose, Avicel, Solka Floc, SO_2-treated wood, and steam-exploded wood, with the highest ethanol yield of 1.8 moles of ethanol per mole of anhydroglucose unit obtained on MN 300 cellulose (28).

A promising near term process development involving C. thermocellum is the Penn/GE system which combines the bacterium with the cellulase producing fungus Thermoactinomyces YX in a single saccharification-fermentation step (30,31). The process involves pretreating poplar chips with hot aqueous butanol to produce a lignin-butanol liquid fuel. The degraded cellulose fraction is then fermented;

however, no provision is made for pentose catabolism. An economic evaluation of the Penn/GE process indicates that ethanol costs are highly dependent on process yield and by-product credits (30).

B. Bacterial Adsorption

The adsorption of bacteria onto solid surfaces has been reported in the literature of several scientific disciplines and extensively reviewed (12,13). The phenomenon has practical value in fermentation technology, waste and water treatment, and clinical microbiology. Most applications of the adsorptive process have involved the purification, resolution, or concentration of microbial cells. Adsorbed cells have been used in immobilized cell reactors to achieve various bioconversions (8,33,34). The metabolic activities of adsorbed cells can be altered due to the accumulation of nutrients or inhibitory materials at the solid-liquid interface.

Mechanisms. Many aspects of microbial attraction to surfaces can be explained in terms of physicochemical principles of colloid science since bacterial cells behave as "living" colloids in solution. Transport to a solid surface can be active as in the case of chemotaxis by motile bacteria or passive which depends on Brownian motion or convection currents. Bacteria nearing the surface of an adsorbent become subject to attractive forces and tend to concentrate there. This has been demonstrated by vivid photomicrographs in which bacterial cells can be seen firmly attached to various surfaces. In particular, microscopic examination has indicated that C. thermocellum cells

associate tightly with cellulose fibers (29). According to the most plausible of present concepts of the mechanism of bacterial adsorption, the process is one of attractive forces overcoming repulsive ones (12, 13,18,43). Short range chemical bonds and longer-range London-van der Waals forces operate in attracting the cell to the surface. Chemical bonds include electrostatic, covalent, and hydrogen bonds. Forces opposing attraction are charge repulsion, van der Waals forces of repulsion, and steric hindrance. The relative importance of each force depends on the bacterial and adsorbent surfaces which are in turn affected by the environmental conditions.

Factors involved in adsorption. The extent and selectivity of adsorption of a specific bacterial cell on an adsorbent cannot be predicted from theoretical considerations. However, numerous empirical investigations have contributed to an understanding of the factors involved in the adsorption process. These factors are outlined in Figure 3. The adsorption behavior of bacterial species towards a specific adsorbent can show marked differences and this has served as a basis for their separation by ion exchange resins (32,46,47). This is due to the chemical nature of the cell wall surface and its charged constituents such as peptides which vary greatly with species, culture age, and culture medium (20). There is no bulk property of the cell wall surface such as gram-staining, the overall charge, or electrophoretic mobility that has been correlated with adsorptive behavior (12).

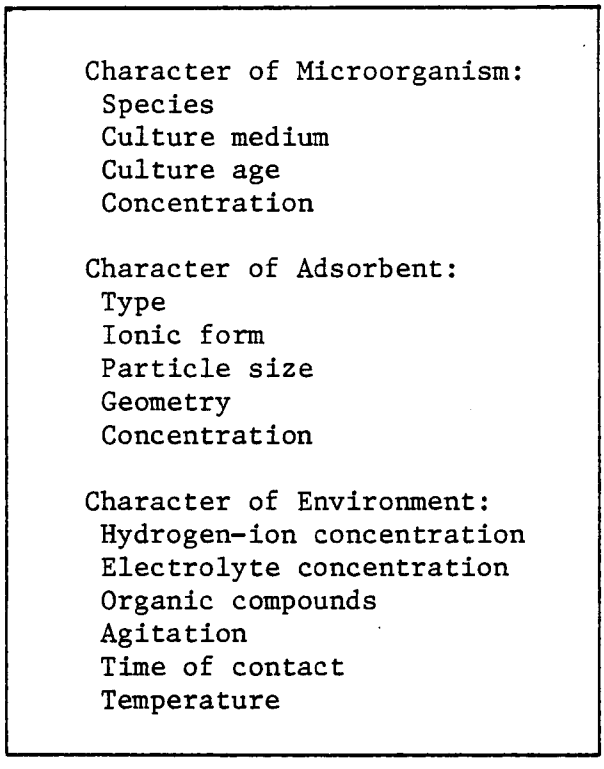

FIGURE 3

Variables Affecting Adsorption of Bacteria on Solid Surfaces[1]

[1]Daniels, S. L., "The Adsorption of Microorganisms onto Solid Surfaces: A Review," Dev. Ind. Microbiol., 13, 211-253 (1972).

The initial concentration of bacterial cells in suspension affects the extent of adsorption and saturation of the adsorbent surface has been observed microscopically.

The nature of the adsorbent is the second most important factor involved in the adsorption process (12,13). Bacteria have been adsorbed to low energy surfaces such as carbons, synthetic polymers, and celluloses; high energy surfaces such as glass, silicas, and aluminas; and a variety of ion exchange resins. All of the attractive and repulsive forces mentioned play some role in the adsorption to these types of adsorbents; however, some generalizations can be made. Low energy surfaces tend to quickly accumulate large numbers of more loosely bound cells, whereas high energy surfaces slowly accumulate smaller numbers of more firmly attached cells (18). Adsorption to activated carbon and other low energy surfaces may involve mostly hydrogen and London-van der Waals forces. Ionic interactions are likely to be more important in adsorption to high energy surfaces since they possess more strongly charged ionizable groups (18). The net surface charge of these nonspecific adsorbents is usually negative as is the case for glasses, clays, soils, activated carbons, and coal (12,18,21,41). Specific and generally reversible adsorption by anion and cation exchange resins is predominantly an electrostatic charge mechanism (12). Bacterial cells behave as charged ions and are capable of exchanging with the mobile ions of the resin. The selectivity of a particular resin has been found to be dependent on the type of exchangeable counter ions suggesting that some complementary

interaction may also be present. However, the affinity of a specific bacterial species for a given ion exchange resin is not predictable. The size and geometry of the adsorbent particles are also important considerations (12). Smaller particles are better adsorbents than larger particles due to greater surface areas. Rough, amorphous surfaces enhance adsorption by also providing fine surface projections which increase the probability of contacting a cell. Increased quantities of adsorbent added to a bacterial suspension increases the degree of adsorption.

The pH and ionic character of the suspending medium influences bacterial adsorption due to the effects on surface constituents of the cell and adsorbent. Bacterial cells have mostly negative charges at physiological pH. According to the Zwitterion hypothesis (12), the bacterial cell can also assume a cationic character if the pH of the solution is below the isoelectric point of the cell surface constituents. This may explain the observation that, in general, the strongest adsorption of bacterial cells occurs at pH 3-6 (12). Adsorption of organic substances from water is also increased with decreasing pH (41). This may be due to the neutralization of negative surface charges on adsorbents by the increasing hydrogen-ion concentration. In some cases, adsorption to ion exchange resins can be reversed completely by altering the pH. The pH for optimum adsorption depends on the relative isoelectric points of the cells and the adsorbent (12). Multivalent cations can enhance adsorption in acid medium by charge reversal and a variety of inorganic salts can promote desorption.

Organic adsorptions are generally exothermic; hence the extent of adsorption generally increases with decreasing temperature (41). This has also been found to be the case for bacterial adsorptions on charcoals (23). Adsorption is generally improved by increased duration and/or intensity of agitation due to increasing the probability of contact; however, optimum conditions may be exceeded which cause desorption (12). Adsorption equilibrium is usually achieved within 15 minutes although several hours has been required in some cases (12).

Adsorption equilibria. Initial attachment of bacteria to a solid surface is a diffusion controlled process and transport coefficients for sorbing bacteria have been determined (12). After some time and at constant temperature, the concentration of cells remaining in solution reaches dynamic equilibrium with that on the surface. Hence, there is a defined distribution of cells between the liquid and solid phases which can be expressed as an adsorption isotherm. The preferred form for depicting the adsorption isotherm is to express the number of adsorbed cells per gram of adsorbent as a function of the concentration of cells in solution.

Several of the classical adsorption isotherms have been used to describe the adsorption of bacteria including the Langmuir (18,21,38), Freundlich (14,37), and a specially devised S-shaped isotherm (23). The Langmuir isotherm is of particular interest since it has been useful in describing monolayer coverage typical of carbon

adsorbents (26). It is expressed:

$$\bar{C}_S = \frac{(\bar{C}_S)_{max} K_1 \bar{C}_L}{1 + K_1 \bar{C}_L} \qquad \text{(III-1)}$$

in which

$\bar{C}_L$ = solute concentration in solution at equilibrium, mass of solute/ml of solution

$\bar{C}_S$ = solute adsorbed per unit weight of adsorbent, mass of solute/g of adsorbent

$(\bar{C}_S)_{max}$ = maximum adsorbable mass per unit weight of adsorbent, mass of solute/g of adsorbent

K_1 = the Langmuir coefficient, ml of solution/mass of solute.

The Langmuir isotherm may be deduced from either kinetic considerations or the thermodynamics of adsorption (2,41). The thermodynamic derivation is based on the assumptions that maximum adsorption corresponds to a saturated monolayer of solute on the adsorbent surface with an infinite concentration of solute in the liquid phase, that the energy of adsorption is constant, and that there is no transmigration of adsorbate in the plane of the surface. Although these assumptions are probably not met in a complex system such as bacteria adsorbing to solids, the Langmuir equation can be useful in quantitatively comparing adsorption behavior for varied conditions within a given system. The value of $(\bar{C}_S)_{max}$, for instance, rarely represents a true monolayer coverage, however, it is indicative of a practical limiting value for

adsorption under the existing conditions. Similarly, K_1 cannot be interpreted in terms of the absolute adsorption energy since it is not a dimensionless quantity.

CHAPTER IV

THEORY

A. Langmuir Adsorption Isotherm

The Langmuir adsorption isotherm for bacteria adsorbing onto a solid surface can be derived from a kinetic analysis analagous to Michaelis-Menten enzyme kinetics. The theory assumes that a liquid phase cell first combines with an adsorption site to form an intermediate. The intermediate then slowly decays in a second step to give a free site and an adsorbed cell. The mechanism can be expressed:

$$C_L + S \underset{k_{-1}}{\overset{k_{+1}}{\rightleftharpoons}} C_L \cdot S \xrightarrow{k_2} C_S + S \qquad \text{(IV-1)}$$

in which

C_L = bacterial concentration in solution, number of cells/ml of solution

S = unoccupied adsorption sites per unit weight of adsorbent, number of sites/g of adsorbent

$C_L \cdot S$ = intermediate defined as liquid phase cells combined with adsorption sites per unit weight of adsorbent, number of sites/g of adsorbent

C_S = bacteria adsorbed per unit weight of adsorbent, number of cells/g of adsorbent.

It is assumed that the rate of decay of intermediate $C_L \cdot S$ to C_S is much slower than that to the reversible step of $C_L \cdot S$ to C_L, i.e.

k_{-1} (and k_{+1}) >> k_2, and that the concentration of cells in solution is much greater than the total number of sites in solution, i.e. C_L >> S_T. The rate of intermediate formation is given by

$$d[C_L \cdot S]/dt = k_1[C_L][S] - (k_{-1} + k_2)\ [C_L \cdot S] \quad . \qquad \text{(IV-2)}$$

The rate of intermediate formation is so quick that an equilibrium is attained instantaneously. At equilibrium, $d[C_L \cdot S]/dt = 0$, and for k_{-1}>> k_2, the Langmuir coefficient is defined by

$$K_1 = k_1/k_{-1} \quad . \qquad \text{(IV-3)}$$

The total number of adsorption sites per unit mass of adsorbent, S_T, is the sum of the occupied and unoccupied sites at equilibrium:

$$[S_T] = [\bar{S}] + [\overline{C_L \cdot S}] \quad . \qquad \text{(IV-4)}$$

Substituting equation IV-4 for $[\bar{S}]$ into equation IV-2 at equilibrium and rearranging results in an expression for the intermediate concentration:

$$[\overline{C_L \cdot S}] = \frac{K_1[\bar{C}_L][S_T]}{1 + K_1[\bar{C}_L]} \quad . \qquad \text{(IV-5)}$$

The second step of the formation of adsorbed cells on the solid surface is

$$\frac{d[C_S]}{dt} = k_2[\overline{C_L \cdot S}] \quad . \qquad \text{(IV-6)}$$

Since k_2 << k_{+1}(or k_{-1}) and the formation of C_S from the intermediate is first order kinetics, one may write

$$[C_S] = K_2[\overline{C_L \cdot S}] \qquad \text{(IV-7)}$$

in which K_2 is a constant proportional to k_2. Substituting equation IV-7 into IV-5 gives

$$[C_S] = \frac{K_1 K_2 [\overline{C}_L] S_T}{1 + K_1 [\overline{C}_L]} \quad . \qquad \text{(IV-8)}$$

If one defines the maximum adsorption of cells as

$$[\overline{C}_S]_{max} = K_2 [S_T] \quad , \qquad \text{(IV-9)}$$

equation IV-8 reduces to

$$\overline{C}_S = \frac{(\overline{C}_S)_{max} K_1 \overline{C}_L}{1 + K_1 \overline{C}_L} \qquad \text{(IV-10)}$$

which is the Langmuir isotherm. Equation IV-10 is the same as the Michaelis-Menten equation in which $\overline{C}_S$ has replaced the rate of product formation and $\overline{C}_L$ has replaced substrate concentration. Expressing the Langmuir equation in double reciprocal form permits the determination of constants K_1 and $(\overline{C}_S)_{max}$ by plotting the inverse of $\overline{C}_S$ against the inverse of $\overline{C}_L$ as in a Lineweaver-Burk plot for the enzyme kinetics. The double reciprocal form obtained from rearrangement of equation IV-10 is

$$\frac{1}{\overline{C}_S} = \frac{1}{K_1 (\overline{C}_S)_{max}} \frac{1}{\overline{C}_L} + \frac{1}{(\overline{C}_S)_{max}} \quad . \qquad \text{(IV-11)}$$

B. Adsorption with Changes in Adsorbate Interaction Potential

As seen from the experimental data presented in Chapter VII, in a double reciprocal plot, there is a breakpoint in each isotherm indicating a departure from the assumptions of the classical Langmuir isotherm. If cells are immobilized on a surface to a certain

concentration, the immobilized cells will interact with free or bound cells in the same neighborhood. For instance, bound cells will exert a repulsive force on the approach of nearby cells in the liquid phase. Therefore, the adsorption free energy has to be modified.

The adsorption equilibrium constant K is the equilibrium coefficient between $\overline{C}_S$ and $\overline{C}_L$ at a given temperature. The free energy change ΔG and the equilibrium constant K for an adsorption process are given by

$$-\Delta G = RT \ln K = RT \ln \frac{\overline{C}_S}{\overline{C}_L} \quad . \qquad \text{(IV-12)}$$

In a lower concentration region, the adsorption potential may be increased due to reduction of repulsive potential since cell concentration is lower. Thus the expression for free energy change in equation IV-12 has to be modified. If one defines the quantities with an asterisk as those quantities for a lower concentration region, then

$$\Delta G^* = \Delta G - \Delta G_I = -RT \ln K^* \qquad \text{(IV-13)}$$

in which ΔG_I is the free energy change caused by a repulsive potential. Equation IV-13 can be rewritten as

$$-RT \ln K + RT \ln K_I = -RT \ln K^* \qquad \text{(IV-14)}$$

from which

$$K^* = K/K_I \quad . \qquad \text{(IV-15)}$$

The contribution to the equilibrium constant due to the reduction in repulsive potential is

$$K_I = \exp(-\Delta G_I/RT) \quad . \qquad \text{(IV-16)}$$

Combining equation IV-15 and IV-16, K and K* are related through ΔG_I by

$$K^* = K \exp(\Delta G_I/RT) \quad . \qquad \text{(IV-17)}$$

A Langmuir adsorption isotherm in a lower concentration region in which K_1^* is substituted for K_1 can be modified by expressing K* as in equation IV-17

$$\frac{\bar{C}_S}{(\bar{C}_S)_{max}} = \frac{K \exp(\Delta G_I)/RT)\ \bar{C}_L}{1 + K \exp(\Delta G_I/RT)\ \bar{C}_L} \quad . \qquad \text{(IV-18)}$$

This equation can be rearranged to the double reciprocal form to give

$$\frac{1}{\bar{C}_S} = \frac{\exp(-\Delta G_I/RT)}{K\ (\bar{C}_S)_{max}} \cdot \frac{1}{\bar{C}_L} + \frac{1}{(C_S)_{max}} \quad . \qquad \text{(IV-19)}$$

If only the linear terms of the series expansion of the exponential term are kept, equation IV-19 becomes

$$\frac{1}{\bar{C}_S} = \frac{1-A}{K\ (\bar{C}_S)_{max}} \cdot \frac{1}{\bar{C}_L} + \frac{1}{(\bar{C}_S)_{max}} \qquad \text{(IV-20)}$$

where

$$A = \Delta G_I/RT \quad . \qquad \text{(IV-21)}$$

In the constant adsorption free energy field at higher concentrations, A = 0, and equation IV-20 reduces to

$$\frac{1}{\bar{C}_S} = \frac{1}{K\ (\bar{C}_S)_{max}} \cdot \frac{1}{\bar{C}_L} + \frac{1}{(\bar{C}_S)_{max}} \qquad \text{(IV-22)}$$

which is equivalent to equation IV-11 for adsorption in the higher concentration region.

A breakpoint in the adsorption isotherm due to the change in interaction potential is analagous to competitive inhibition of enzyme kinetics in the Lineweaver-Burk plot. The abscissa intercepts for equations IV-20 and IV-22 are, respectively, $-K/(1-A)$ and $-K$. The parameter A can then be determined by extrapolation from the two adsorption regions. This concept is illustrated in Figure 4. For adsorption data that indicate that this dual mechanism occurs, the value of ΔG_I can be determined to quantitatively describe the change in adsorbate interaction potential.

C. Effect of Temperature on Equilibrium Constant

Enthalpies of adsorption, ΔH, may be evaluated from temperature coefficients of the equilibrium constant K following van't Hoff's equation

$$\left(\frac{\partial \ln k}{\partial T}\right)_P = \frac{\Delta H}{RT^2} \quad . \tag{IV-23}$$

Using the relation

$$d(1/T) = -dT/T^2 \quad , \tag{IV-24}$$

equation IV-23 becomes

$$\left(\frac{\partial \ln k}{d(1/T)}\right)_P = -\frac{\Delta H}{R} \quad . \tag{IV-25}$$

Substituting equation IV-12 into equation IV-25, results in

$$\frac{d(\Delta G/T)}{d(1/T)} = \Delta H \quad . \tag{IV-26}$$

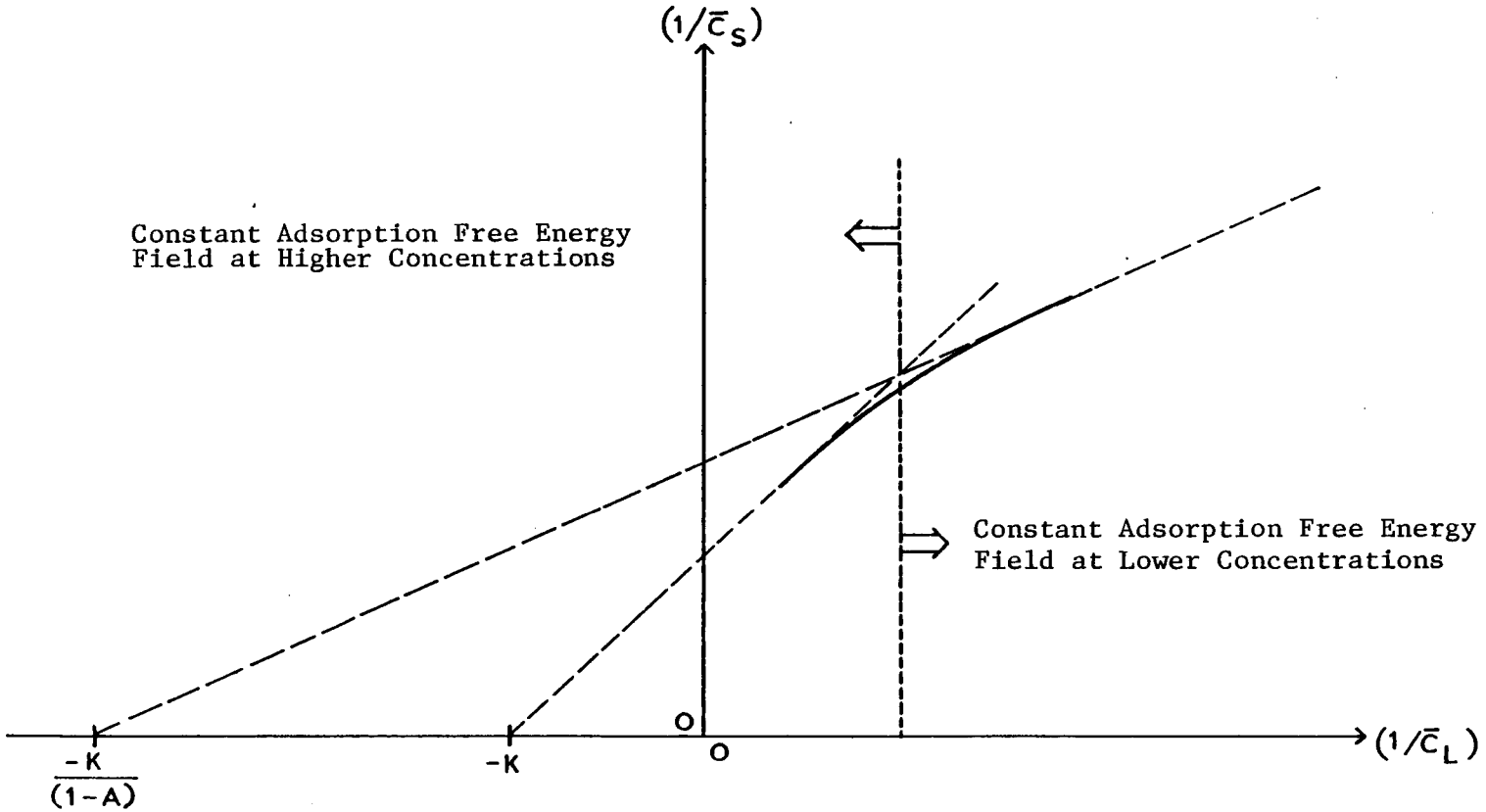

FIGURE 4

Schematic Diagram Showing the Double Reciprocal Plot of
Langmuir Adsorption and its Modification

Differentiating equation IV-26 and using the following relationship in the result

$$\left(\frac{\partial(\Delta G)}{\partial T}\right)_P = -\Delta S \qquad \text{(IV-27)}$$

gives

$$\ln K = -\Delta H/RT + \Delta S/R \quad . \qquad \text{(IV-28)}$$

The values of ΔH and ΔS for adsorption with repulsive interactions can be calculated when K is available at several temperatures. For an adsorption process with a reduction in repulsive potential, a similar treatment results in

$$\ln K^* = -\Delta H^*/RT + \Delta S^*/R \quad . \qquad \text{(IV-29)}$$

The effect of the reduction in interaction potential on these thermodynamic properties can then be determined from

$$\Delta H = \Delta H^* + \Delta H_I \qquad \text{(IV-30)}$$

$$\Delta S = \Delta S^* + \Delta S_I \quad . \qquad \text{(IV-31)}$$

CHAPTER V

MATERIALS AND EXPERIMENTAL PROCEDURES

A. Microorganism Maintenance

Microorganism. Clostridium thermocellum ATCC 27405 (4) obtained from the American Type Culture Collection (Rockville, MD) was utilized in the experimentation.

Culture medium. The composition of the culture medium was that modified by Garcia-Martinez et al. (17) from the CM3 medium of Weimer and Zeikus (42). The modified CM3 medium contained (g/l): KH_2PO_4,1.5; K_2HPO_4,2.9; $(NH_4)_2SO_4$,1.3; $MgCl_2 \cdot 6H_2O$, 1.0; $CaCl_2 \cdot 2H_2O$,0.15; yeast extract (Difco Laboratories, Detroit, MI), 2.0; cysteine hydrochloride hydrate, 1.0; $FeSO_4 \cdot 6H_2O$,1.25 mg/l; and 1 ml of a 0.2% (w/v) resazurin (Kodak, Rochester, NY) aqueous solution. The cellobiose (Kodak) concentration was 1.0% (w/v) which served as the carbon source. The procedures recommended by the VPI Anaerobe Laboratory for preparation of prereduced anaerobically sterilized (PRAS) media were followed (15). The pH was adjusted with 8N NaOH or 5N HCl to 7.0 before sterilization. For plating, 2.0% (w/v) agar was added to the medium prior to sterilization.

Growth of microorganism. The bacteria were cultivated in 16 x 125 mm Hungate type anaerobic culture tubes (Bellco, Vineland, NJ) and in petri dishes placed in anaerobic jars (BBL, Cockeysville, MD) using Gas-paks (BBL) for anaerobiosis.

The working volume of the Hungate tubes was 10 ml and transfers were made using the syringe method (26). The medium was autoclaved in two portions in Hungate tubes: a 1.0% (w/v) cysteine solution and a 9 ml solution containing the rest of the components suspended in 90% of the final volume. After sterilization, 1 ml of the cysteine solution was added to the 9 ml aliquots and the complete medium preincubated in a water bath at 60°C. Anaerobic conditions as indicated by the resazurin dye color change (pink to colorless) were reached after approximately 5 minutes. The medium was then innoculated with 0.5-1.0 ml of log phase bacteria and the culture temperature maintained at 60°C by a dry incubator.

To cultivate the bacteria in petri dishes, 12 ml of the 90% final volume medium with agar in Hungate tubes were sterilized and 1.5 ml of the cysteine solution added. The plates were innoculated with 1 ml of a bacterial culture dilution and the reduced medium poured and mixed. The plates were placed in anaerobic jars, medium side down, and allowed to incubate for 4-6 days at 60°C.

Stock cultures were prepared in Hungate tubes by growing a cell population on 10 ml of the reduced medium. They were maintained by transferring approximately 0.5 ml of a less than 24 hour old culture to 10 ml of fresh medium. Viable cultures were also preserved for several months by storage in a refrigerator at 4°C.

Growth and cell number estimation. Growth was estimated as optical density at 525 nm utilizing a Gilford Model 240 spectrophotometer with an uninnoculated medium sample serving as the blank. The slit width

of the spectrophotometer, which refers to the width of the emitted spectrum, was adjusted to the value necessary for a zero absorbance reading of the blank. The number of cells in solution was determined by developing a calibration curve of viable colony count expressed as cell/ml versus absorbance. The count was estimated by serial dilution and plating of culture samples for which absorbance had been determined (9). The diluents consisted of 9 ml of a 0.1% peptone solution with resazurin and 1 ml of a 1% cysteine solution in Hungate tubes. Transfers of 1 ml were made by the syringe method. Samples of the desired dilution were plated in petri dishes and incubated in anaerobic jars as described. Only plates with 30-300 colonies were counted. The assumption that one viable cell results in one colony was made.

B. Adsorption Experiments

The adsorbent investigated was bituminous coal obtained from the reserves at The University of Tennessee power plant facilities. The coal was pulverized and sieved to a particle size of 0.150-0.180 mm diameter (80/100 Tyler mesh), washed several times with deionized water, and dried at 100°C for 24 hours. To conduct an experiment, known and equal weights of coal were placed in two Hungate tubes. The weight of coal used from one experiment to another ranged between 0.12 g and 0.15 g. Cells used for the experiment were obtained by centrifugation of approximately 12 hour old cultures at 5,000 g for 10 minutes. The supernatant was decanted and the cells resuspended to the desired cell concentration in fresh CM3 medium. Five ml of the cell suspension were added to the first coal sample and 5 ml of uninnoculated medium

were added to the second which served as the control. The remaining cell suspension and uninnoculated media were used for an absorbance measurement of the original cell concentration. The pH of the two coal suspensions were adjusted to the desired value and agitated in a Dubnoff metabolic shaking incubator at the desired temperature for 20 minutes. Temperature was maintained by circulation of water from a Haake constant temperature bath. The suspensions were allowed to settle for several minutes and a sample of each supernatant filtered through a Sweeney filter with a metal screen which retained coal particles but allowed free passage of cells. These samples were used for an absorbance measurement of the equilibrium cell concentration.

CHAPTER VI

RESULTS

A. Cell Growth

Growth in a batch system. C. thermocellum was grown in Hungate tubes containing 15 ml of modified CM3 medium. Approximately 1.5 ml of the culture were taken by syringe and monitored for absorbance at 525 nm and for pH at several time intervals until growth ceased. The growth curve and pH of the culture over the course of growth on cellobiose are presented in Figure 5 and the experimental data are tabulated in Table A-I of the Appendix. The maximum specific growth rate of 0.19 hr^{-1}, which indicated a maximum doubling time of 3.7 hr, was maintained over the first 12 hours of growth. Culture growth ceased after about 30 hours of growth and was accompanied by a decrease in culture pH from 7.0 to 5.15.

Estimation of cellular concentration by absorbance. The viable colony count and absorbance at 525 nm for cultures grown for various lengths of time are correlated in Figure 6. Linear regression was used to fit the experimental data (see Table A-II of the Appendix) to the equation

$$\text{Colony Count} \times 10^{-6}, \text{ (cell/ml)} = 114 \times \text{Absorbance (525 nm)} - 3.93 \quad \text{(VI-1)}$$

with a correlation coefficient of 0.961. Since cultures used were in the growth stage, cell death did not significantly affect the correlation. However, systematic deviations were noted which caused the ordinate intercept to be less than zero.

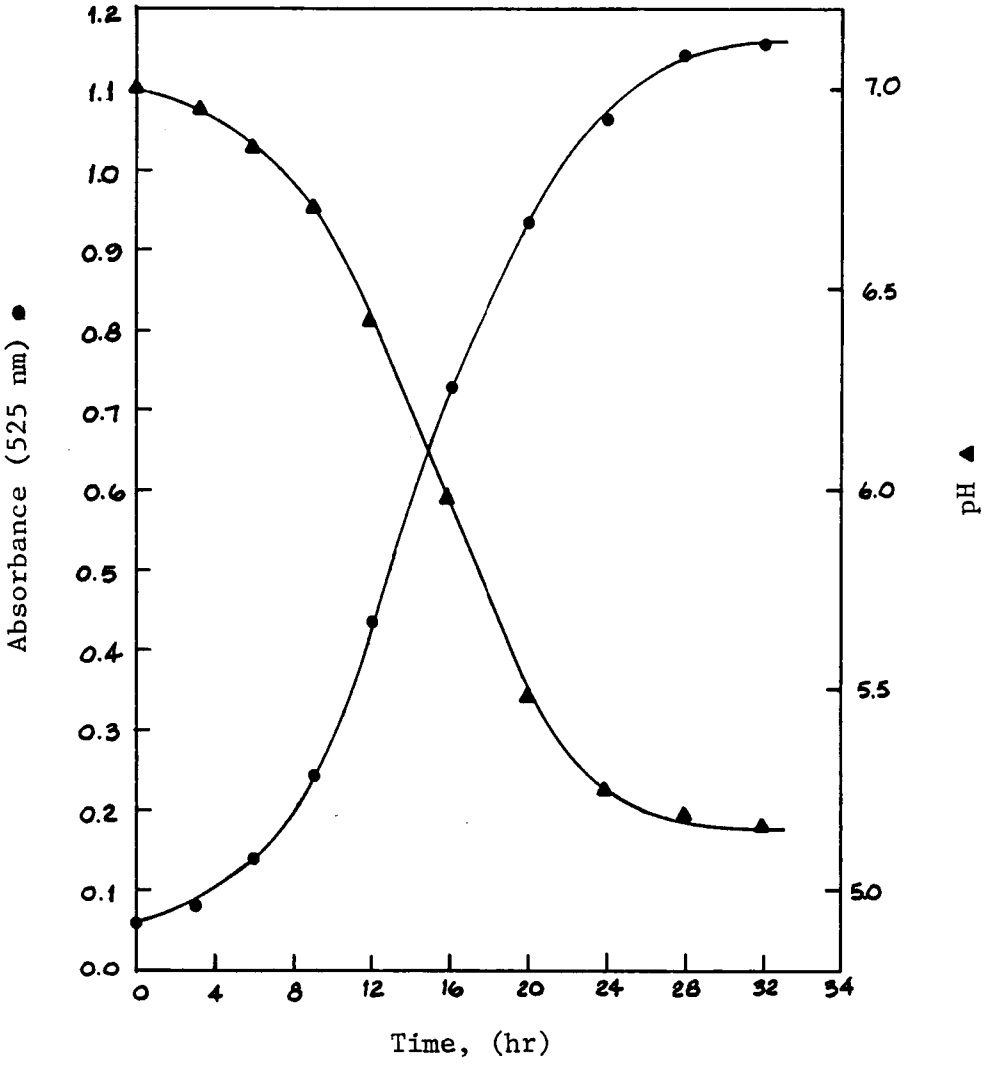

FIGURE 5

Growth and pH Variation of Clostridium thermocellum Culture Grown on Cellobiose with Time

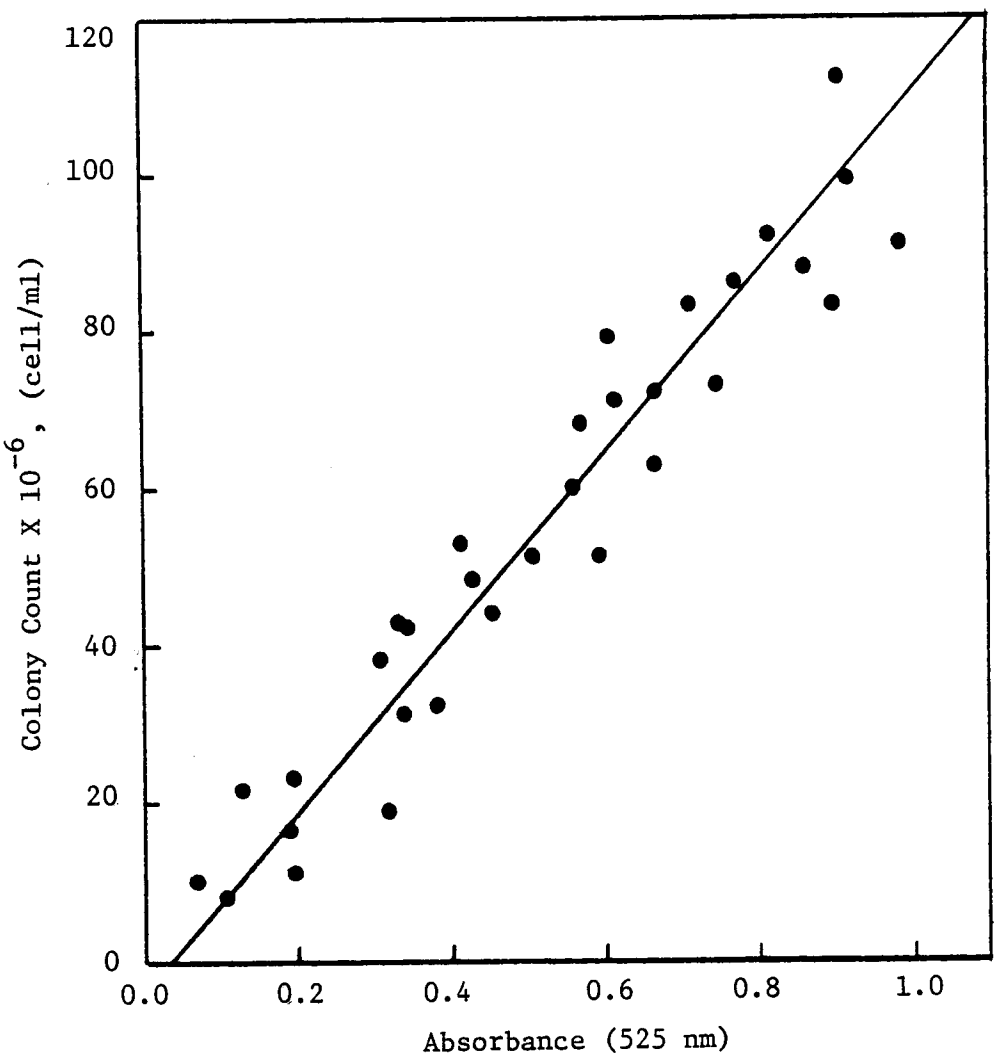

FIGURE 6

Calibration Curve Between Viable Colony Count and Culture Absorbance at 525 nm

B. Adsorption Experiments

Time required for equilibria. Initial adsorption experiments were conducted at 60°C and 7.0 pH in order to determine the time required for adsorption equlibrium. The number of cells adsorbed per gram of coal was obtained from a cell balance before and after adsorption expressed by:

$$\bar{C}_S = \frac{(C_L - \bar{C}_L)\ V}{m} \qquad \text{(VI-2)}$$

in which

m = mass of adsorbent, g

V = volume of cellular suspension = 5 ml.

C_L and $\bar{C}_L$ were obtained from, respectively, initial and final absorbance values of the cellular suspension using equation VI-1. Values for $\bar{C}_S$ were obtained for contact times of 10, 20, 40 and 60 minutes using two liquid phase cellular concentrations. The results are presented in Figure 7 which indicated that equilibrium was reached in approximately 20 minutes for both liquid concentrations. Experimental data are given in Tables A-III and A-IV of the Appendix. Since the doubling time of the bacteria was much longer than the time required for an adsorption experiment, cell reproduction did not significantly affect the results.

Adsorption isotherms at selected temperatures. The adsorption isotherms of C. thermocellum cells on coal particles were constructed by determining the solid phase cellular concentrations as a function of liquid phase cellular concentrations at equilibrium through

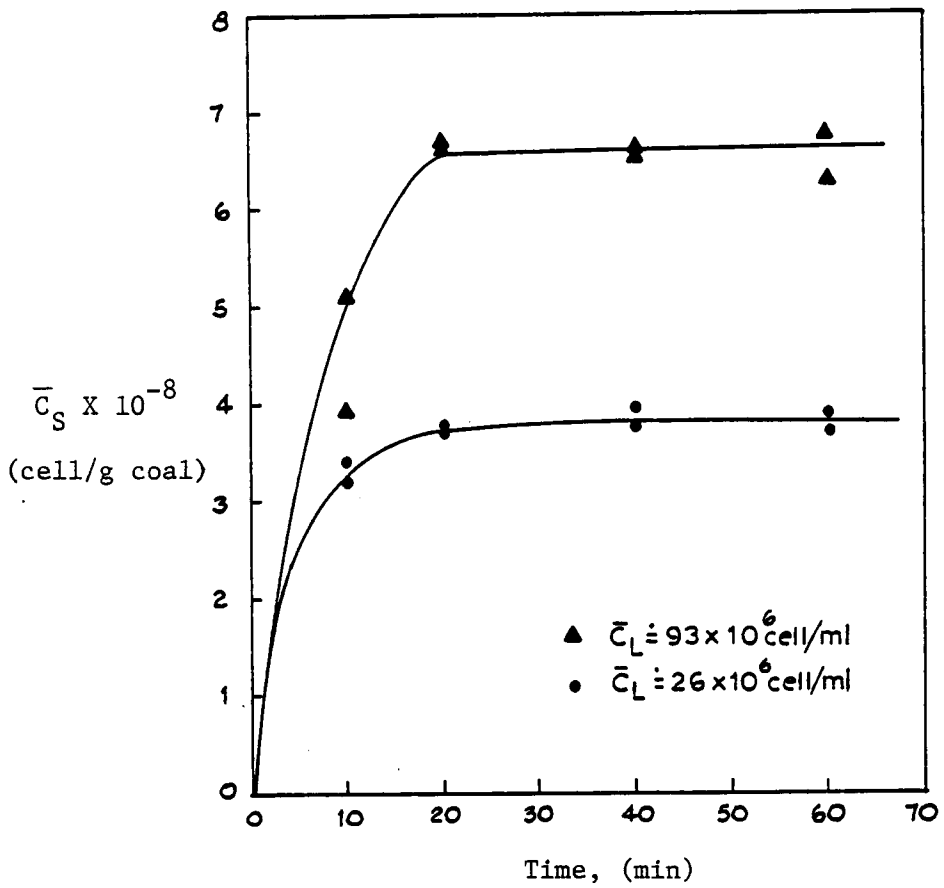

FIGURE 7

Variations of Immobilized Cell Concentration on Coal Particles with Respect to Time at 60°C and 7.0 pH

equation VI-2. Isothermal data were collected for a pH value of 7.0 and temperatures of 60°C, 45°C, and 30°C. These data are presented in Table I, Table II, and Table III. The isotherms, the equilibrium concentrations of each phase at a given temperature, are plotted in Figure 8 as $\bar{C}_S$ versus $\bar{C}_L$. Adsorption increased as temperature decreased and more so between 45°C and 30°C than between 60°C and 45°C.

Adsorption isotherms at selected pH Values. The effect of pH on adsorption was investigated by developing two additional isotherms at 60°C, one at 6.0 pH and another at 5.0 pH. The data for these isotherms are given in Table IV and Table V. The range of pH values used (7.0-5.0) was that encountered in batch growth of C. thermocellum. Figure 9 illustrates the effect of pH on the isotherms. The lower pH values significantly increased adsorption especially at higher values of $\bar{C}_L$.

TABLE I

ADSORPTION ISOTHERM DATA--60°C, 7.0 pH

Weight of Coal (g)	Initial Absorbance at 525 nm	$C_L \times 10^{-6}$ (cell/ml)	Equilibrium Absorbance at 525 nm	$\bar{C}_L \times 10^{-6}$ (cell/ml)	$\bar{C}_S \times 10^{-8}$ (cell/g)
0.145	0.253	24.9	0.171	15.5	3.24
0.149	0.243	23.8	0.157	14.0	3.29
0.138	0.359	37.0	0.266	26.4	3.83
0.143	0.358	36.9	0.263	26.0	3.82
0.137	0.423	44.3	0.323	32.9	4.15
0.141	0.504	53.5	0.386	40.1	4.74
0.143	0.517	55.0	0.400	41.6	4.68
0.152	0.499	52.9	0.381	39.5	4.41
0.137	0.680	73.6	0.538	57.4	5.91
0.139	0.651	70.3	0.524	55.8	5.21
0.142	0.812	88.6	0.668	72.2	5.79
0.130	0.833	91.0	0.700	75.8	5.84
0.137	0.878	96.1	0.717	77.8	6.68
0.136	0.894	98.0	0.750	81.5	6.05
0.145	1.001	110.1	0.832	90.9	6.63
0.144	1.017	112.0	0.848	92.7	6.71
0.131	1.068	117.8	0.936	102.7	5.75
0.137	1.101	121.5	0.945	103.8	6.47
0.136	1.260	139.7	1.103	121.8	6.57
0.140	1.305	144.8	1.152	127.4	6.21

TABLE II

ADSORPTION ISOTHERM DATA--45°C, 7.0 pH

Weight of Coal (g)	Initial Absorbance at 525 nm	$C_L \times 10^{-6}$ (cell/ml)	Equilibrium Absorbance at 525 nm	$\bar{C}_L \times 10^{-6}$ (cell/ml)	$\bar{C}_S \times 10^{-8}$ (cell/g)
0.147	0.256	25.2	0.149	13.0	4.15
0.149	0.271	26.9	0.166	15.0	3.98
0.141	0.287	28.8	0.184	17.0	4.20
0.146	0.304	30.7	0.199	18.8	4.07
0.142	0.395	41.1	0.273	27.2	4.88
0.150	0.460	48.5	0.319	32.4	5.38
0.141	0.536	57.2	0.393	40.8	5.83
0.143	0.649	70.0	0.500	53.1	5.91
0.145	0.809	88.3	0.638	68.8	6.72
0.141	1.190	131.7	0.803	87.6	7.38
0.136	1.186	131.2	0.994	109.3	8.04
0.137	1.263	140.0	1.059	116.8	8.45
0.131	1.301	144.3	1.112	122.8	8.21

TABLE III

ADSORPTION ISOTHERM DATA--30°C, 7.0 pH

Weight of Coal (g)	Initial Absorbance at 525 nm	$C_L \times 10^{-6}$ (cell/ml)	Equilibrium Absorbance at 525 nm	$\bar{C}_L \times 10^{-6}$ (cell/ml)	$\bar{C}_S \times 10^{-8}$ (cell/g)
0.140	0.279	27.9	0.148	12.9	5.35
0.135	0.291	29.2	0.156	13.9	5.68
0.142	0.321	32.7	0.182	16.8	5.59
0.131	0.364	37.5	0.219	21.0	6.29
0.137	0.553	59.1	0.359	37.0	8.06
0.129	0.608	65.4	0.421	44.1	8.26
0.138	0.865	94.6	0.615	66.2	10.3
0.127	1.109	122.5	0.862	94.3	11.1
0.126	1.226	135.8	0.996	109.6	10.4

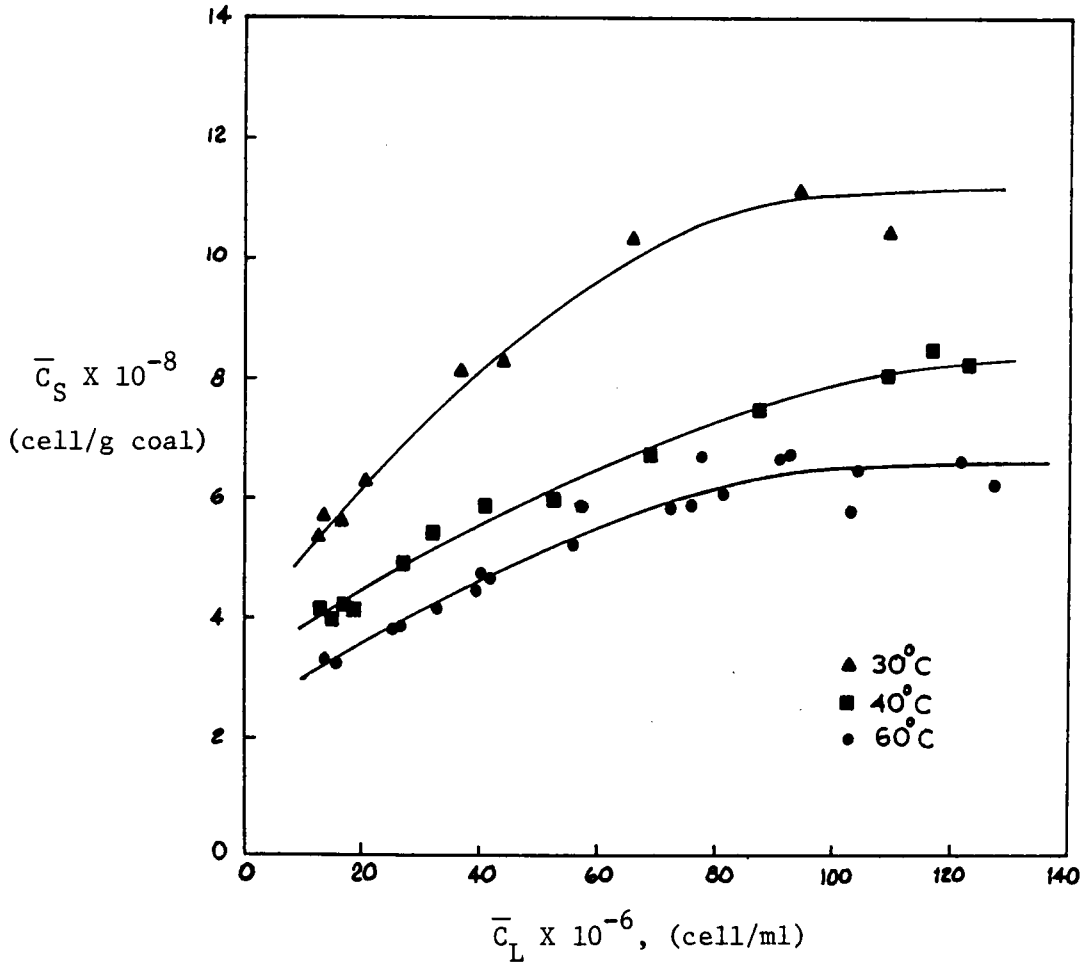

FIGURE 8

Adsorption Isotherms of Clostridium thermocellum Cells on Coal Particles at 60°C, 45°C, and 30°C with 7.0 pH

TABLE IV

ADSORPTION ISOTHERM DATA--60°C, 6.0 pH

Weight of Coal (g)	Initial Absorbance at 525 nm	$C_L \times 10^{-6}$ (cell/ml)	Equilibrium Absorbance at 525 nm	$\bar{C}_L \times 10^{-6}$ (cell/ml)	$\bar{C}_S \times 10^{-8}$ (cell/g)
0.146	0.278	27.8	0.164	14.7	4.50
0.142	0.335	34.4	0.202	19.1	5.38
0.141	0.372	38.5	0.241	23.5	5.32
0.148	0.443	46.6	0.282	28.2	6.21
0.139	0.515	54.8	0.362	37.3	6.29
0.142	0.649	70.0	0.476	50.3	6.94
0.137	0.860	94.1	0.648	69.9	8.85
0.135	0.880	96.4	0.685	74.1	8.26
0.139	1.044	115.0	0.785	85.5	10.6
0.135	1.075	118.6	0.847	92.6	9.62
0.132	1.365	151.6	1.098	121.2	11.5

TABLE V

ADSORPTION ISOTHERM DATA--60°C, 5.0 pH

Weight of Coal (g)	Initial Absorbance at 525 nm	$C_L \times 10^{-6}$ (cell/ml)	Equilibrium Absorbance at 525 nm	$\overline{C}_L \times 10^{-6}$ (cell/ml)	$\overline{C}_S \times 10^{-8}$ (cell/g)
0.139	0.291	29.2	0.155	13.7	5.56
0.141	0.342	35.0	0.189	17.6	6.17
0.134	0.376	38.9	0.230	22.3	6.21
0.137	0.440	46.2	0.273	27.2	6.94
0.130	0.562	60.1	0.390	40.5	7.52
0.134	0.635	68.4	0.441	46.3	8.26
0.131	0.705	76.4	0.507	53.8	8.62
0.123	0.831	90.8	0.570	61.0	12.1
0.126	0.900	98.6	0.665	71.9	10.6
0.121	1.067	117.7	0.785	85.5	13.3

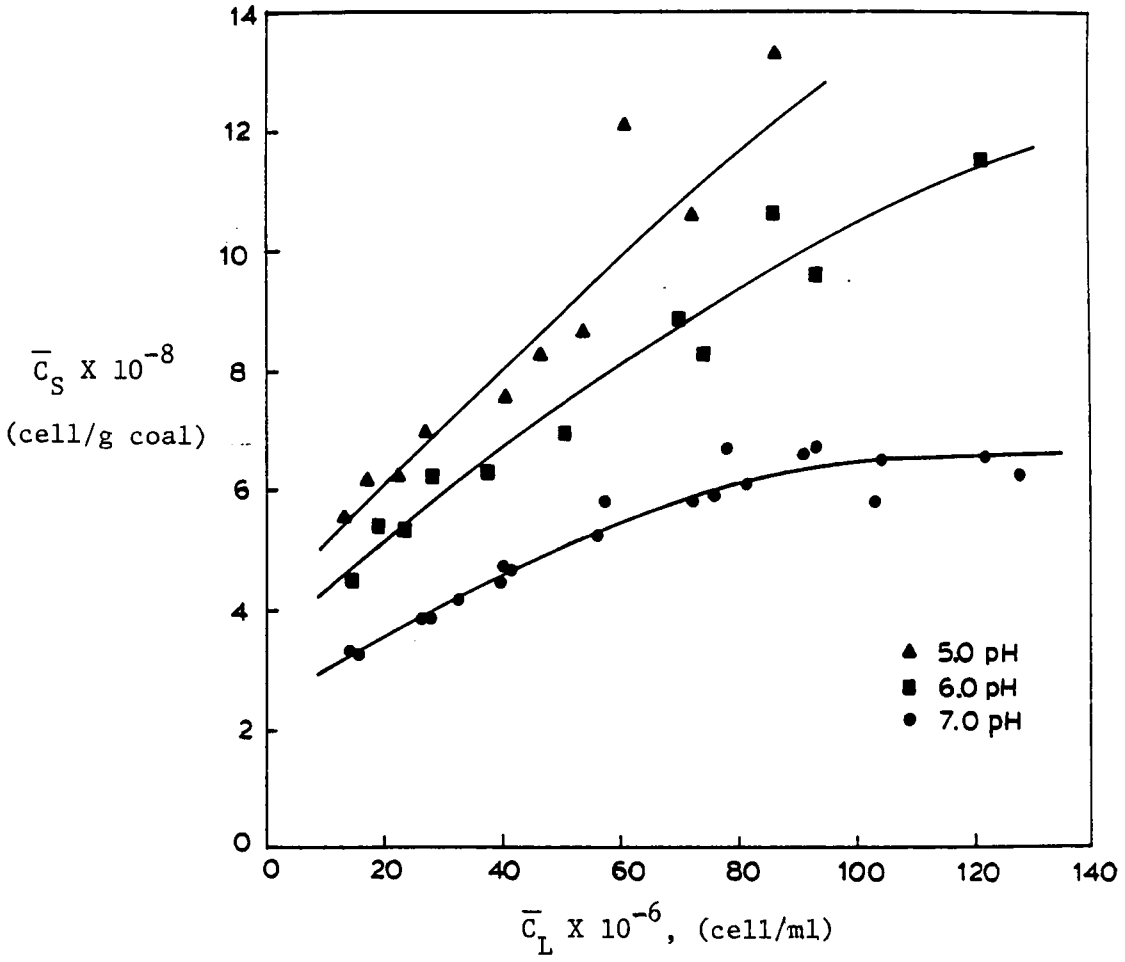

FIGURE 9

Adsorption Isotherms of Clostridium thermocellum Cells on Coal Particles at 60°C with 7.0 pH, 6.0 pH, and 5.0 pH

CHAPTER VII

ANALYSIS AND DISCUSSION OF RESULTS

The adsorption isotherms presented in Figures 8 and 9 for C. thermocellum cells on bituminous coal particles suggested that some adsorption limit was reached at high values of $\bar{C}_L$. Therefore, the isothermal data were analyzed in the double reciprocal form in order to test for conformity with the Langmuir model for adsorption.

A. Isothermal Parameters at Selected Temperatures

The double reciprocal plots for the adsorption data at 60°C, 45°C, and 30°C are presented in Figure 10. A breakpoint occurred in each isotherm indicating nonuniformity of adsorbate interaction potentials over the range of liquid phase cellular concentrations used. For liquid concentrations at or above $(\bar{C}_L)_{trans}$ (trans is for transition) and the corresponding $(\bar{C}_S)_{trans}$, adsorption followed the Langmuir model with a constant adsorbate interaction potential. At concentrations less than $(\bar{C}_L)_{trans}$, a reduction in the repulsive interaction potential was evident. The isotherms in these two regions followed relatively straight lines, hence the characteristic parameters K_1 and $(\bar{C}_S)_{max}$ as defined by equation IV-11 were determined independently. The parameters are tabulated in Table VI for the three isothermal adosrptions. The results of linear regression analysis which was used to fit the data are listed in Table A-V of the Appendix.

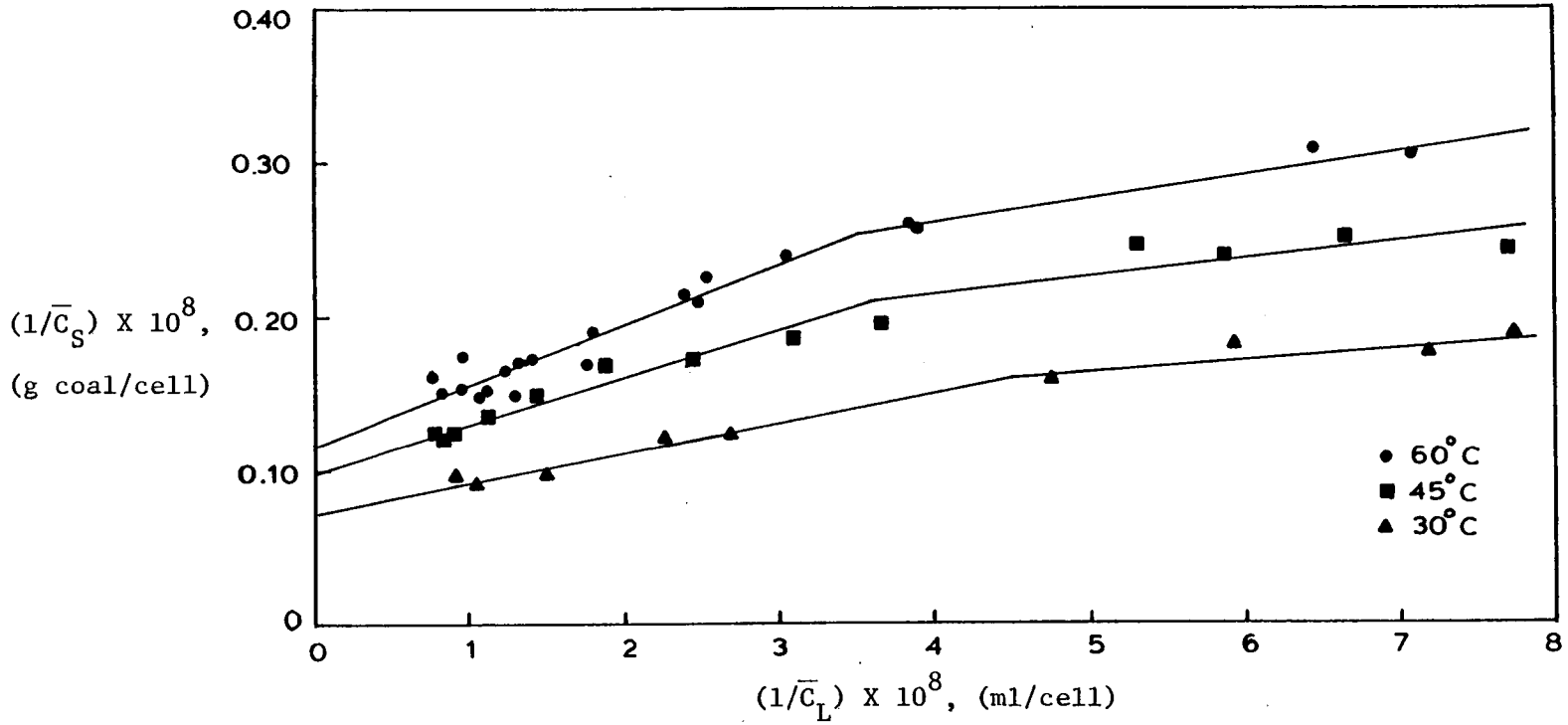

FIGURE 10

Double Reciprocal Plot of Adsorption Isotherms of Clostridium thermocellum Cells on Coal Particles at 60°C, 45°C, and 30°C with 7.0 pH

TABLE VI

EFFECT OF TEMPERATURE ON ADSORPTION ISOTHERM PARAMETERS

Temperature (°C)	Low Equilibrium Concentrations		Transition Concentrations		High Equilibrium Concentrations	
	K_1^* (ml/cell)	$(\bar{C}_S)^*_{max}$ (cell/g)	$(\bar{C}_L)_{trans}$ (cell/ml)	$(\bar{C}_S)_{trans}$ (cell/g)	K_1 (ml/cell)	$(\bar{C}_S)_{max}$ (cell/g)
60	12.4×10^{-8}	5.05×10^{8}	2.83×10^{7}	3.94×10^{8}	3.04×10^{-8}	8.49×10^{8}
45	14.4×10^{-8}	6.00×10^{8}	2.77×10^{7}	4.80×10^{8}	3.31×10^{-8}	10.0×10^{8}
30	16.2×10^{-8}	7.97×10^{8}	2.21×10^{7}	6.23×10^{8}	3.76×10^{-8}	13.7×10^{8}

$K_1 = \frac{k_1}{k_{-1}}$

The values for $(\bar{C}_S)^*_{max}$ in Table VI were used only to define the isotherms at low cellular concentrations and should not be confused with the maximum adsorption limit which is given by $(\bar{C}_S)_{max}$. Maximum adsorption increased with decreasing temperature which is characteristic of exothermic adsorptions. The equilibrium parameters for the high concentration region, K_1, were less than those for low concentrations, K_1^*, at each temperature. This was the result of the surface of the adsorbent being less crowded in the low concentration region thereby reducing repulsive potential to adsorption.

B. Temperature Effect on Equilibrium Coefficients

In order to interpret the data in terms of adsorption energy, the Langmuir coefficients K_1 were converted to the dimensionless equilibrium coefficients K for the three isotherms. The equilibrium coefficient defined in equation IV-12 is proportional to the Langmuir coefficient defined in euqation IV-3. The equilibrium coefficient should be a dimensionless quantity that may be expressed as:

$$K = K_1/k_o \quad . \qquad \text{(VII-1)}$$

The constant k_o has the same units as K_1, i.e. ml/cell. It was used to negate the units of $\bar{C}_L$ and as a proportionality constant for conversion to a molar quantity in the estimation of adsorption energies. Using the relation

$$K = \exp(-\Delta G/RT) \qquad \text{(VII-2)}$$

in equation VII-1, the Langmuir coefficient can be expressed as:

$$K_1 = k_o K = k_o \exp(-\Delta G/RT) \quad . \qquad \text{(VII-3)}$$

Equation VII-3 can be rearranged to give

$$\ln K_1 = -\Delta G/RT + \ln k_o \quad . \qquad \text{(VII-4)}$$

If the free energy of adsorption remains constant over a small temperature change, k_o can be obtained from the Langmuir coefficients of the isotherms. Similarly, the equilibrium coefficient for adsorption in the lower cellular concentration region, K* , is proportional to the isothermal parameter, K_1^* ,

$$K^* = K_1^*/k_o^* \quad . \qquad \text{(VII-5)}$$

Expressing K^* in terms of ΔG^* in equation VII-5 results in

$$K_1^* = k_o^* K^* = k_o^* \exp(-\Delta G^*/RT) \qquad \text{(VII-6)}$$

which after rearrangement gives

$$\ln K_1^* = -\Delta G^*/RT + \ln k_o^* \qquad \text{(VII-7)}$$

Based on equations VII-4 and VII-7, the isothermal equilibrium parameters were plotted as $\ln K_1$ and $\ln K_1^*$ versus inverse absolute temperature in Figure 11. The data were fitted with equations by linear regression analysis which gave

$$\ln K_1 = 708/T - 19.4 \text{ [=] ml/cell}, \ \sigma = 0.11 \text{ ml/cell} \qquad \text{(VII-8)}$$

$$\ln K_1^* = 873/T - 18.5 \text{ [=] ml/cell}, \ \sigma = 0.13 \text{ ml/cell} \qquad \text{(VII-9)}$$

in which σ is the standard deviation. The values of k_o and k_o^*, determined from equations VII-8 and VII-9, were found to be

$$k_o = 3.61 \times 10^{-9} \text{ ml/cell} \qquad \text{(VII-10)}$$

$$k_o^* = 9.13 \times 10^{-9} \text{ ml/cell} \qquad \text{(VII-11)}$$

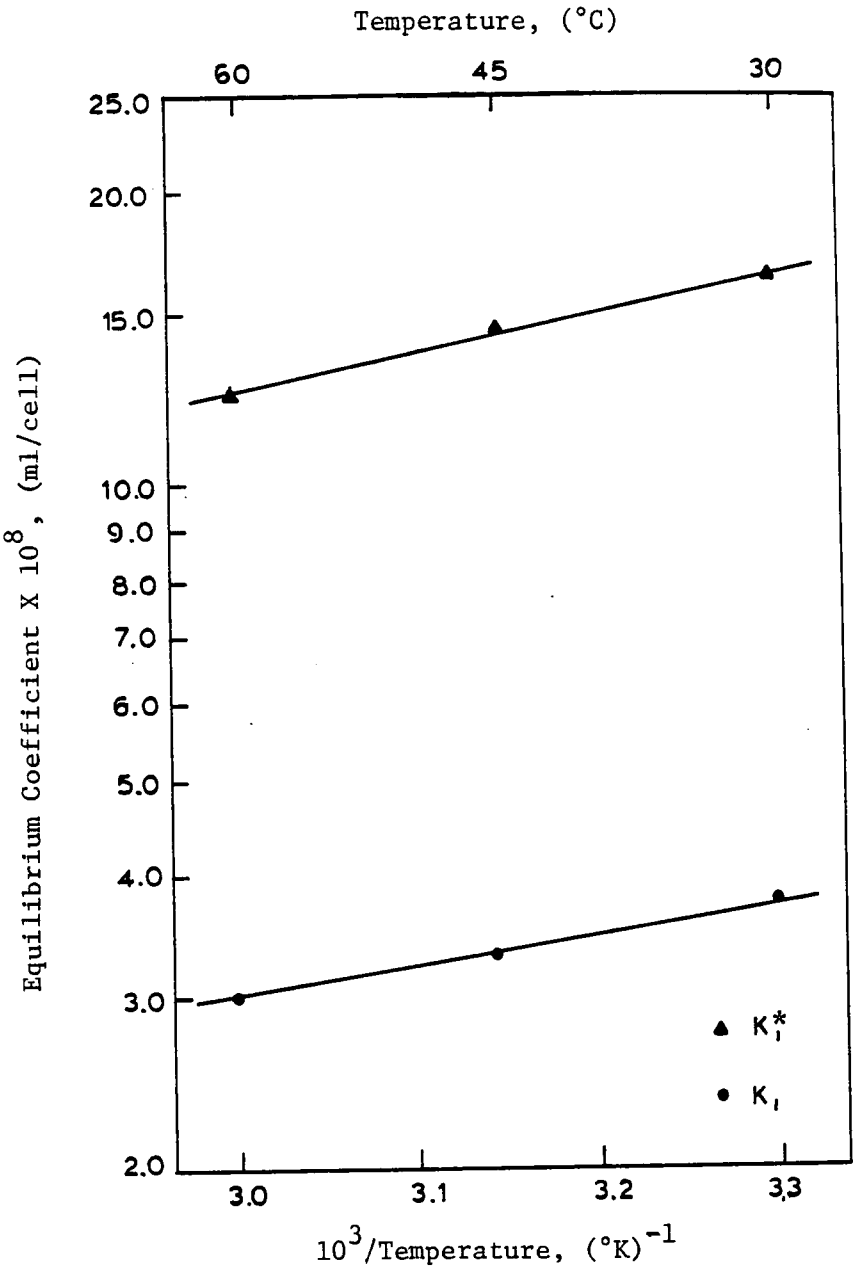

FIGURE 11

Equilibrium Coefficients Defined by Equation IV-11
as a Function of Temperature

The equilibrium coefficients for each concentration region were determined from the isothermal parameters using the values of k_o and k_o^* in equations VII-1 and VII-6. From equation IV-15, the contribution to the equilibrium coefficient K^* due to the reduction in repulsive potential, K_I, is the ratio of K-to-K^*. The values of K, K^*, and K_I were expressed as the free energy changes, ΔG, ΔG^*, and ΔG_I as in equation IV-14. The equilibrium coefficients and their associated free energy changes are presented in Table VII for the three temperatures. The value of the gas constant used in equation IV-14 was 1.987 cal/gmol°K.

Negative values for ΔG and ΔG^* were indicative of thermodynamically favorable adsorption in both regions of cellular concentration. Adsorptions in the lower concentration region were more favorable than those at higher concentrations since the magnitude of ΔG^* is greater than that of ΔG and K^* is greater than K at each temperature. The positive value of ΔG_I and values of K_I less than unity were attributed to increasing repulsion between cells at higher equilibrium concentrations.

In order to determine the enthalpy and entropy changes of adsorption, equilibrium coefficients in the form lnK and $\ln K^*$ were plotted against inverse absolute temperature based on equations IV-29 and IV-30. These plots are presented in Figure 12. Linear regression analysis gave

$$\ln K = 719/T - 0.033, \ \sigma = 0.107 \qquad \text{(VII-12)}$$

$$\ln K^* = 896/T - 0.076, \ \sigma = 0.134 \ . \qquad \text{(VII-13)}$$

Values for enthalpies and entropies of adsorption for the two

TABLE VII

EFFECT OF TEMPERATURE ON EQUILIBRIUM CONSTANTS
AND GIBBS FREE ENERGY CHANGES

Temperature (°C)	Low Equilibrium Concentrations		High Equilibrium Concentrations		Adsorbate Interaction	
	K*	ΔG* (Kcal/gmol)	K	ΔG (Kcal/gmol)	K_I	ΔG_I (Kcal/gmol)
60	13.6	-1.73	8.42	-1.41	0.619	+0.32
45	15.8	-1.74	9.17	-1.40	0.580	+0.34
30	17.7	-1.73	10.4	-1.41	0.588	+0.32

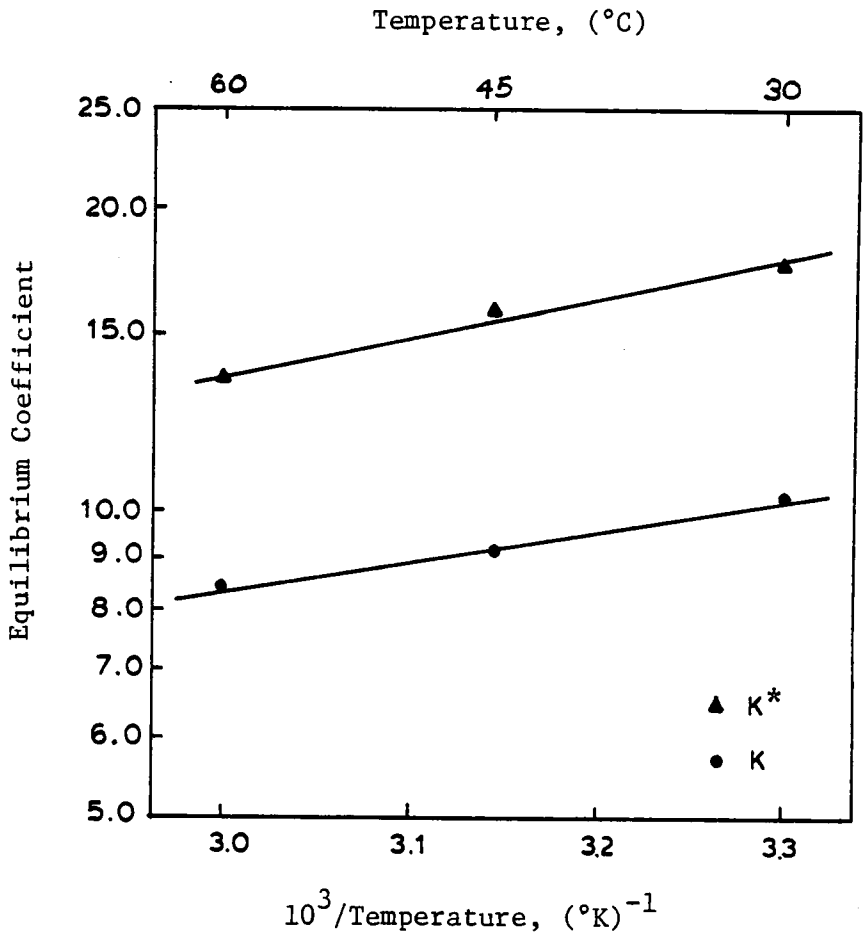

FIGURE 12

Equilibrium Coefficients Defined by Equations VII-1 and VII-5 as a Function of Temperature

concentration regions were determined from, respectively, the slopes and ordinate intercepts as shown in equations VII-12 and VII-13. The effect of the change in repulsive potential on these thermodynamic quantities was expressed as ΔH_I and ΔS_I through equations IV-30 and IV-31. The results are given below:

Adsorption Enthalpies	Adsorption Entropies
$\Delta H = -1.43$ Kcal/gmol	$\Delta S = -0.067$ cal/gmol°K
$\Delta H^* = -1.78$ Kcal/gmol	$\Delta S^* = -0.152$ cal/gmol°K
$\Delta H_I = +0.35$ Kcal/gmol	$\Delta S_I = +0.085$ cal/gmol°K

Observed negative values for ΔH and ΔH^* indicate that bacterial uptake on the coal particles in both concentration environments was exothermic. Thus the decrease of temperature results in increased adsorption, or a shift of equilibria in the exothermic direction, which is in accord with Le Chaterlier's principle. Adsorption was more exothermic in the lower concentration region. The positive ΔH_I value was a result of the increased repulsive potential caused by larger populations of adsorbed cells at higher concentrations. The magnitudes of the heats of adsorption, ΔH and ΔH^*, were relatively small indicating predominance of a physical adsorption process.

The quantities of ΔS and ΔS^* were small negative values which indicate that some external work was required for adsorption. The external work input to the process may be identified as chemotaxis by the bacteria, agitation of the coal-bacteria suspensions, and heat input to the system.

C. Effect of pH on Isothermal Parameters and Adsorption Free Energy

The data for the isotherms at 60°C with pH values of 7.0, 6.0, and 5.0 were expressed in the double reciprocal form. These isotherms are presented in Figure 13. A breakpoint in the isotherms was again apparent. The isothermal parameters for these pH values were also determined for the two concentration regions. These parameters are presented in Table VIII for the isothermal adsorptions. Table A-V of the Appendix contains also the results of the linear regression analysis used to fit the isotherms at pH values of 6.0 and 5.0.

The decrease in pH value of the bacterial suspension has a dramatic effect on maximum adsorption, $(\overline{C}_S)_{max}$. This was possibly a result of neutralization of negative surface charges on the cells and coal particles by increased hydrogen-ion concentrations. However, the Langmuir coefficients K_1 decreased as the pH value decreased from 7.0 to 5.0. Further, the region of transition of adsorbate interaction potential shifted to higher values of $\overline{C}_L$ (and $\overline{C}_S$) at the lower pH values.

The equilibrium coefficients, K and K^*, as defined by equations VII-1 and VII-5 were determined using the constants k_o and k_o^* given in equations VII-10 and VII-11. Values of K_I and the free energy changes associated with each equilibrium coefficient were also calculated. These quantities are presented in Table IX for the isotherms at 60°C and the selected pH values.

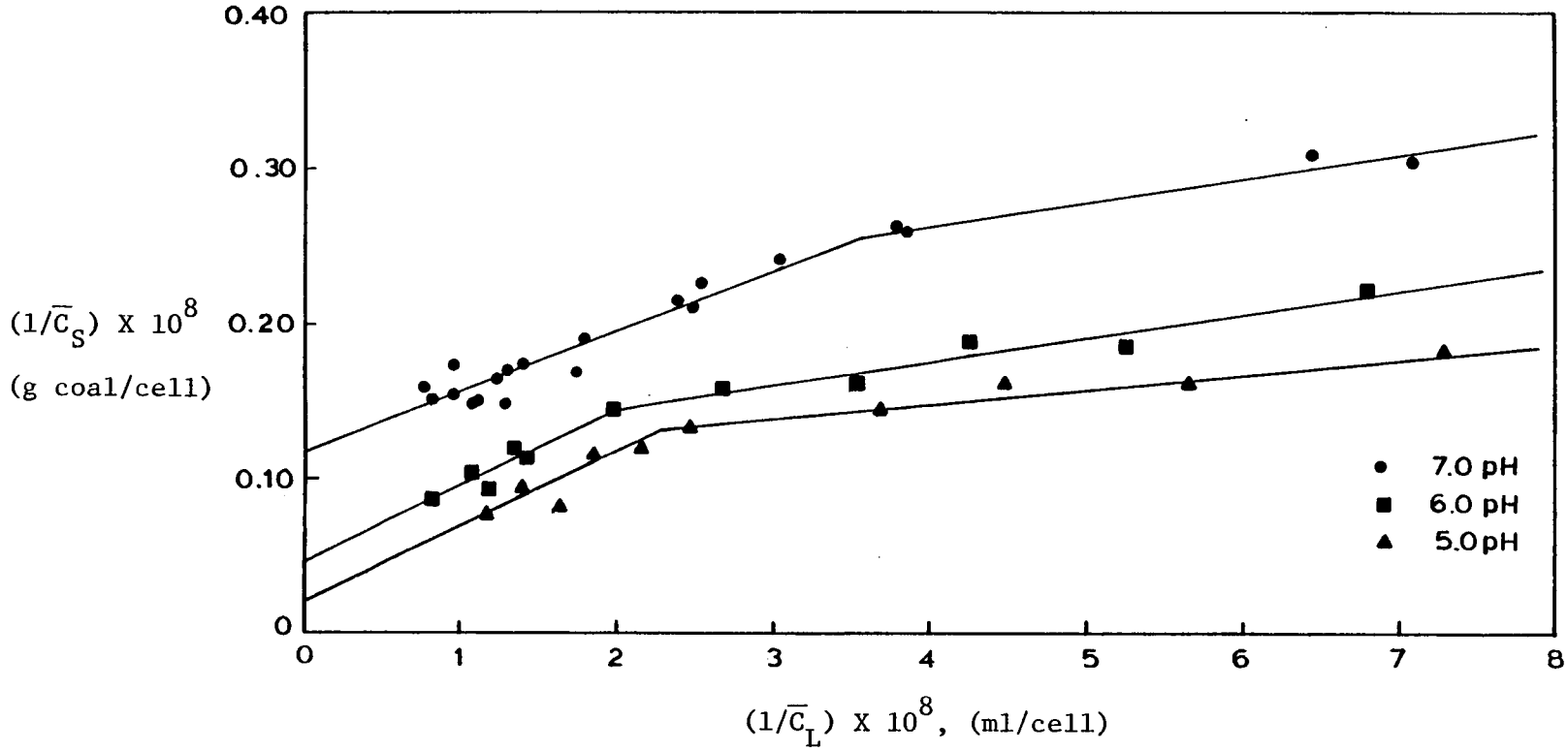

FIGURE 13

Double Reciprocal Plot of Adsorption Isotherms of Clostridium thermocellum Cells on Coal Particles at 60°C with 7.0 pH, 6.0 pH, and 5.0 pH

TABLE VIII

EFFECT OF pH ON ADSORPTION
ISOTHERM PARAMETERS

	Low Equilibrium Concentrations		Transition Concentrations		High Equilibrium Concentrations	
pH	K_1^* (ml/cell)	$(\bar{C}_S)^*_{max}$ (cell/g)	$(\bar{C}_L)_{trans}$ (cell/ml)	$(\bar{C}_S)_{trans}$ (cell/g)	K_1 (ml/cell)	$(\bar{C}_S)_{max}$ (cell/g)
7.0	12.4×10^{-8}	5.05×10^{8}	2.83×10^{7}	3.94×10^{8}	3.04×10^{-8}	8.49×10^{8}
6.0	7.38×10^{-8}	8.80×10^{8}	5.05×10^{7}	6.93×10^{8}	0.909×10^{-8}	22.0×10^{8}
5.0	11.7×10^{-8}	9.00×10^{8}	4.31×10^{7}	7.51×10^{8}	0.497×10^{-8}	44.0×10^{8}

TABLE IX

EFFECT OF pH ON EQUILIBRIUM CONSTANTS
AND GIBBS FREE ENERGY CHANGES

	Low Equilibrium Concentrations		High Equilibrium Concentrations		Adsorbate Interaction	
pH	K*	ΔG^* (Kcal/gmol)	K	ΔG (Kcal/gmol)	K_I	ΔG_I (Kcal/gmol)
7.0	13.6	-1.73	8.42	-1.41	0.619	+0.32
6.0	8.12	-1.39	2.52	-0.61	0.310	+0.78
5.0	12.9	-1.69	1.38	-0.21	0.107	+1.48

Repulsive interactions were much greater in the higher concentration region than at lower concentrations for the isotherms at pH values of 6.0 and 5.0. This was evident from the large positive values of ΔG_I and from the decrease in values for K at lower pH values. The increase in repulsive potential was due to higher cell populations on the coal particles at lower pH values. The negative values of ΔG and ΔG^* indicated that adsorption was promising at all three pH values. However, the lower magnitude of ΔG at lower pH values suggested adsorption was less favorable in thermodynamic terms.

CHAPTER VIII

CONCLUSIONS

The adsorption isotherms of C. thermocellum cells on bituminous coal particles were determined at selected temperatures and pH values. From the analysis of the isotherms in the double reciprocal form, the following conclusions were drawn:

1. The isothermal adsorptions can be correlated with a modified Langmuir isotherm which accounts for a reduction in repulsive interactions at low cellular concentrations.
2. The isothermal parameter for maximum adsorption, $(\overline{C}_S)_{max}$, indicated a capacity of 8.5×10^8 cell/g for the coal particles at 60°C and 7.0 pH. Maximum adsorption increased with decreasing temperature and with decreasing pH value.
3. Equilibrium coefficients were determined from the adsorption isotherm parameters. Observed negative values of free energy change indicated adsorption was thermodynamically favorable and more so at lower cellular concentrations.
4. Temperature coefficients of the equilibrium constant at 60°C, 45°C, and 30°C, and a pH value of 7.0, established that adsorption was exothermic. Exothermicity of adsorption increased at low cellular concentrations.
5. Small, negative values for entropy of adsorption indicated that some external work was necessary for the adsorption process to occur.

6. The effect of reduction in pH value at 60°C was to increase adsorption which may be due to neutralization of negative surface charges on the cells and coal particles. However, for adsorptions at the pH values of 6.0 and 5.0, the results indicated less thermodynamically favorable adsorption at high immobilized cell concentrations due to increased repulsive potentials.

LIST OF REFERENCES

LIST OF REFERENCES

1. Abbott, B. J., "Immobilized Cells," in Annual Reports on Fermentation Processes, D. Perlman, ed. (Academic Press, New York, 1977), Vol. 1, pp. 205-233.

2. Adamson, A. W., Physical Chemistry of Surfaces, 3rd ed. (Wiley-Interscience, New York, 1976).

3. Ait, N., N. Creuzet, and P. Forget, "Partial Purification of Cellulase from Clostridium thermocellum," J. Gen. Microbiol., 113, 399-402 (1979).

4. American Type Culture Collection, 13th ed. (American Type Culture Collection, Rockville, MD, 1974).

5. Brock, T. D., Biology of Microorganisms, 2nd ed. (Prentice-Hall, Englewood Cliffs, 1974), p. 715.

6. Brooks, R., T. M. Su, M. Brennan, and J. Frick, "Bioconversion of Plant Biomass to Ethanol," in Proceedings of the 3rd Annual Biomass Energy Systems Conference (Solar Energy Research Institute, Department of Energy, Golden, CO, 1979), p. 275.

7. Bu'Lock, J. D., "Industrial Alcohol," in Microbial Technology: Current State, Future Prospects, A. T. Bull, D. C. Ellwood, and C. Ratledge, eds. (Cambridge University Press, Cambridge, 1979), p. 309.

8. Chibata, I. and T. Tosa, "Transformations of Organic Compounds by Immobilized Microbial Cells," in Advances in Applied Microbiology, D. Perlman, ed. (Academic Press, New York, 1977), Vol. 22, pp. 1-27.

9. Collins, C. H. and P. M. Lyne, Microbiological Methods, 4th ed. (Butterworths, London, 1976), p. 197.

10. Cooney, C. L., D. I. C. Wang, S. Wang, J. Gordon, and M. Jiminez, "Simultaneous Cellulose Hydrolysis and Ethanol Production by a Cellulolytic Anaerobic Bacterium," Biotechnol. Bioeng. Symp. No. 8, 103-114 (1978).

11. Cooney, C. L. and D. L. Wise, "Thermophilic Anaerobic Digestion of Solid Waste for Fuel Gas Production," Biotechnol. Bioeng., 17, 1119-1135 (1975).

12. Daniels, S. L., "Mechanisms Involved in Sorption of Microorganisms to Solid Surfaces," in Adsorption of Microorganisms to Surfaces, G. Bitton and K. C. Marshall, eds. (Wiley-Interscience, New York, 1980), pp. 7-58.

13. Daniels, S. L., "The Adsorption of Microorganisms onto Solid Surfaces: A Review," Dev. Ind. Microbiol., 13, 211-253 (1972).

14. DeNicola, K., and D. J. Kirwan, "Adsorption Isotherms of Azotobacter vinelandii on Cellex E," Biotechnol. Bioeng., 22, 1283-1286 (1980).

15. Dowell, V. R. and T. M. Hawkins, Laboratory Methods in Anaerobic Bacteriology (U.S. Government Printing Office, Washington, 1974).

16. Flickinger, M. C., "Current Biological Research in Conversion of Cellulosic Carbohydrates into Liquid Fuels: How Far Have We Come?" Biotechnol. Bioeng., 22, Suppl. 1, 27-48 (1980).

17. Garcia-Martinez, D. V., A. Shinmyo, A. Madia, and A. L. Demain, "Studies on Cellulase Production by Clostridium thermocellum," Eur. J. Appl. Microbiol. Biotechnol., 9, 189-197 (1980).

18. Gerson, D. F. and J. E. Zajic, "The Biophysics of Cellular Adhesion," in Immobilized Microbial Cells, K. Venkatsubramanian, ed. (American Chemical Society, Washington, 1979), pp. 29-57.

19. Herrero, A. A. and R. F. Gomez, "Development of Ethanol Tolerance in Clostridium thermocellum: Effect of Growth Temperature," Appl. Environ. Microbiol., 40, 571-577 (1980).

20. Jack, T. R. and J. E. Zajic, "The Immobilization of Whole Cells," in Advances in Biochemical Engineering, T. K. Ghose, T. A. Fiechter, and N. Blackbrough, eds. (Springer-Verlag, Berlin, 1977), Vol. 5, pp. 125-145.

21. Khairnar, D. R., "The Effect of Chemical Competition on Thermodynamics of Bacterial Adsorption," Ph.D. thesis, Utah State University, Logan, 1971; Diss. Abstr. Int. B, 32, (7), 3732 (1972).

22. Kipling, J. J., Adsorption from Solutions of Non-Electrolytes (Academic Press, New York, 1965).

23. Krishnamurti, K., "Studies in the Adsorption of Bacteria," Proc. Indian Acad. Sci., B34, 81-91 (1951).

24. Lamed, R., and J. G. Zeikus, "Ethanol Production by Thermophilic Bacteria: Relationship Between Fermentation Product Yields of and Catabolic Enzyme Activities in Clostridium thermocellum and Thermoanaerobium brockii," J. Bacteriol., 144, 569-578 (1980).

25. Lilly, M. D. and P. Dunnill, "Biochemical Reactors," Process Biochem., 6, 29-32 (1971).

26. Macey, J. M., J. E. Snellen, and R. E. Hungate, "Use of Syringe Methods for Anaerobiosis," American J. Clin. Nutrit., 25, 1318-1323 (1972).

27. McBee, R. H., "The Characteristics of Clostridium thermocellum," J. Bacteriol., 67, 505-506 (1954).

28. Ng, T. K., A. Ben-Bassat, and J. G. Zeikus, "Ethanol Production by Thermophilic Bacteria: Fermentation of Cellulosic Substrates by Cocultures of Clostridium thermocellum and Clostridium thermohydrosulfuricum," Appl. Environ. Microbiol., 41, 1337-1343 (1981).

29. Ng, T. K., P. J. Weimer, and J. G. Zeikus, "Cellulolytic and Physiological Properties of Clostridium thermocellum," Arch. Microbiol., 114, 1-7 (1977).

30. Pye, E. K. and A. E. Humphrey, "Production of Liquid Fuels from Cellulosic Biomass," in Proceedings of the 3rd Annual Biomass Energy Systems Conference (Solar Energy Research Institute, Department of Energy, Golden, CO, 1979), p. 69.

31. Remirez, R., "Wood-to-Ethanol Methods Edge Closer to Fruition," Chem. Eng., 88, No. 2, 51-55 (1981).

32. Rotman, B., "Uses of Ion Exchange Resins in Microbiology," Bacteriol. Rev., 24, 251-260 (1960).

33. Scott, C. D., and C. W. Hancher, "Use of a Tapered Fluidized Bed as a Continuous Bioreactor," Biotechnol. Bioeng., 18, 1393-1403 (1976).

34. Seyhan, E., and D. J. Kirwan, "Nitrogenase Activity of Immobilized Azotobacter vinelandii," Biotechnol. Bioeng., 21, 271-281 (1979).

35. Shinmyo, A., D. V. Garcia-Martinez, and A. L. Demain, "Studies on the Extracellular Cellulolytic Enzyme Complex Produced by Clostridium thermocellum," J. Appl. Biochem., 1, 202-209 (1979).

36. Sitton, O. C., and J. L. Gaddy, "Ethanol Production in an Immobilized-Cell Reactor," Biotechnol. Bioeng., 22, 1735-1748 (1980).

37. Thomas, C. J., T. A. McMeekin, and C. Balis, "Retention of Bacteria in Liquid Films at Agar Surfaces," Appl. Environ. Microbiol., 34, 456-457 (1977).

38. Van Duuren, F. A., "Removal of Micro-Particles from Water by Coagulation," Water Treat. Exam., 18, 128-149 (1969).

39. Vieth, W. R., and K. Venkatsubramanian, "Immobilized Microbial Cells in Complex Biocatalysis," in Immobilized Microbial Cells, K. Venkatsubramanian, ed. (American Chemical Society, Washington, 1979), pp. 1-11.

40. Wang, D. I. C., I. Biocic, H. Y. Fang, and S. D. Wang, "Direct Microbiological Conversion of Cellulosic Biomass to Ethanol," in Proceedings of the 3rd Annual Biomass Energy Systems Conference (Solar Energy Research Institute, Department of Energy, Golden, CO, 1979), p. 61.

41. Weber, W. J., Jr., "Adsorption," in Physicochemical Processes for Water Quality Control, W. J. Weber, Jr., ed. (Wiley-Interscience, New York, 1972), pp. 199-259.

42. Weimer, P. J., and J. G. Zeikus, "Fermentation of Cellulose and Cellobiose by Clostridium thermocellum in the Absence and Presence of Methanobacterium thermoautotrophicum," Appl. Environ. Microbiol., 33, 289-297 (1977).

43. Weiss, L., "A Biophysical Consideration of Cell Contact Phenomena," in Adhesion in Biological Systems, R. S. Manly, ed. (Academic Press, New York, 1970), pp. 1-14.

44. Zeikus, J. G., "Chemical and Fuel Production By Anaerobic Bacteria," Ann. Rev. Microbiol., 34, 423-464 (1980).

45. Zeikus, J. G., "Thermophilic Bacteria: Ecology, Physiology and Technology," Enzyme Microb. Technol., 1, 243-252 (1979).

46. Zvyagintsev, D. G., "Some Regularities of Adsorption of Microorganisms on Ion Exchange Resins," Mikrobiologiya, 31, 339-343 (1960).

47. Zvyagintsev, D. G. and V. S. Guzev, "Concentration and Separation of Bacteria on Dowex Anionite," Mikrobiologiya, 40, 139-143 (1971).

APPENDIX

TABLE A- I

EXPERIMENTAL DATA FOR GROWTH AND pH VARIATION OF CULTURE GROWN ON CELLOBIOSE WITH TIME

Time (hr)	Absorbance at 525 nm	Slit Width (mm)	pH
0	0.055	0.020	7.00
3	0.080	0.020	6.95
6	0.138	0.020	6.85
9	0.241	0.020	6.70
12	0.428	0.020	6.42
16	0.725	0.020	5.98
20	0.933	0.020	5.48
24	1.062	0.021	5.25
28	1.143	0.020	5.18
32	1.155	0.020	5.15

TABLE A-II

EXPERIMENTAL DATA FOR VIABLE COLONY COUNT VERSUS ABSORBANCE[a]

Absorbance at 525 nm	Slit Width (mm)	Colony Count X 10^{-6} (cell/ml)	Number of Plates Counted
0.069	0.017	10.1	6
0.105	0.021	8.0	5
0.123	0.021	21.6	2
0.186	0.019	16.7	4
0.191	0.020	11.0	5
0.196	0.023	23.9	3
0.308	0.019	38	4
0.317	0.019	18.9	3
0.330	0.017	43	4
0.338	0.018	31	5
0.343	0.016	42	6
0.382	0.021	32	4
0.410	0.016	53	5
0.429	0.022	48	5
0.452	0.019	44	4
0.507	0.019	51	5
0.554	0.022	60	4
0.570	0.015	68	3
0.593	0.021	51	4
0.605	0.017	79	5
0.614	0.023	71	3
0.665	0.021	63	5
0.688	0.019	72	4
0.712	0.022	83	4
0.746	0.019	73	3
0.769	0.017	86	2
0.813	0.020	92	4
0.860	0.018	88	3
0.895	0.020	83	4
0.905	0.020	112	5
0.917	0.019	99	4
0.983	0.021	91	3

[a] Correlation coefficient = 0.961.

TABLE A- III

EXPERIMENTAL DATA FOR ADSORPTION AS A FUNCTION OF TIME AT LOW EQUILIBRIUM CONCENTRATIONS

Time (min)	Weight of Coal (g)	Initial Absorbance at 525 nm	Slit Width (mm)	$C_L \times 10^{-6}$ (cell/ml)	Final Absorbance at 525 nm	Slit Width (mm)	$\bar{C}_L \times 10^{-6}$ (cell/ml)	$\bar{C}_S \times 10^{-8}$ (cell/g)
10	0.144	0.355	0.021	36.5	0.273	0.025	27.2	3.22
10	0.146	0.365	0.020	37.7	0.278	0.023	27.8	3.40
20	0.138	0.359	0.021	37.0	0.266	0.021	26.4	3.83
20	0.143	0.358	0.017	36.9	0.263	0.019	26.0	3.82
40	0.139	0.348	0.018	35.7	0.256	0.026	25.2	3.76
40	0.142	0.352	0.022	36.2	0.254	0.030	25.0	3.94
60	0.143	0.358	0.017	36.9	0.265	0.031	26.3	3.71
60	0.142	0.354	0.019	36.4	0.257	0.033	25.4	3.89

TABLE A-IV

EXPERIMENTAL DATA FOR ADSORPTION AS A FUNCTION OF TIME AT HIGH EQUILIBRIUM CONCENTRATIONS

Time (min)	Weight of Coal (g)	Initial Absorbance at 525 nm	Slit Width (mm)	$C_L \times 10^{-6}$ (cell/ml)	Final Absorbance at 525 nm	Slit Width (mm)	$\bar{C}_L \times 10^{-6}$ (cell/ml)	$\bar{C}_S \times 10^{-8}$ (cell/g)
10	0.148	0.972	0.022	106.9	0.870	0.021	95.2	3.94
10	0.139	0.985	0.021	108.3	0.860	0.020	94.1	5.09
20	0.145	1.001	0.020	110.1	0.832	0.023	90.9	6.63
20	0.144	1.017	0.019	112.0	0.848	0.025	92.7	6.71
40	0.142	0.999	0.017	109.9	0.836	0.031	91.4	6.51
40	0.146	1.024	0.016	112.8	0.853	0.027	93.3	6.67
60	0.142	0.982	0.020	108.0	0.825	0.034	90.1	6.29
60	0.147	1.020	0.021	112.3	0.845	0.031	92.4	6.78

TABLE A-V

LINEAR REGRESSION DATA FOR DOUBLE RECIPROCAL PLOTS OF ADSORPTION ISOTHERMS

Adsorption Isotherm Temperature (°C)	pH	Number of Data Sets	Slope (g/ml)	Ordinate Intercept (g/cell)	Variance[a] ($g^2/cell^2$)	Standard Deviation[a] (g/cell)	Correlation Coefficient
Low Equilibrium Concentrations							
60	7.0	5	1.59×10^{-2}	1.98×10^{-9}	7.03×10^{-20}	2.97×10^{-10}	0.975
45	7.0	5	1.15×10^{-2}	1.67×10^{-9}	4.04×10^{-20}	2.25×10^{-10}	0.776
30	7.0	4	7.76×10^{-3}	1.25×10^{-9}	1.04×10^{-20}	1.18×10^{-10}	0.880
60	6.0	6	1.54×10^{-2}	1.14×10^{-9}	6.49×10^{-20}	2.79×10^{-10}	0.970
60	5.0	5	9.52×10^{-3}	1.11×10^{-9}	2.62×10^{-20}	1.81×10^{-10}	0.974
High Equilibrium Concentrations							
60	7.0	15	3.87×10^{-2}	1.18×10^{-9}	5.97×10^{-20}	2.53×10^{-10}	0.915
45	7.0	8	3.01×10^{-2}	9.96×10^{-10}	5.94×10^{-20}	2.60×10^{-10}	0.966
30	7.0	5	1.94×10^{-2}	7.28×10^{-10}	1.96×10^{-20}	1.57×10^{-10}	0.956
60	6.0	5	4.99×10^{-2}	4.54×10^{-10}	1.52×10^{-20}	1.38×10^{-10}	0.863
60	5.0	5	4.57×10^{-2}	2.27×10^{-10}	3.26×10^{-20}	2.02×10^{-10}	0.878

[a] Variance and standard deviation of ordinate values ($1/\bar{C}_S$).

VITA

Paul Nicholson Horne was born in Jackson, Tennessee, August 8, 1955, to Mr. and Mrs. Paul J. Horne. He attended public schools in Martin, Tennessee and was graduated from Westview High School in May, 1973. The following August he entered Vanderbilt University, and in May, 1978 he received a Bachelor of Arts degree in Molecular Biology.

He entered the Graduate School at The University of Tennessee in September, 1978 to pursue undergraduate and graduate course work in Chemical Engineering. While there, he served as a graduate assistant in the Department of Chemical, Metallurgical and Polymer Engineering. He expects to receive the Master of Science degree in Chemical Engineering in March, 1982. After graduation, Mr. Horne will be employed with the Buckeye Cellulose Corporation in Memphis, Tennessee.